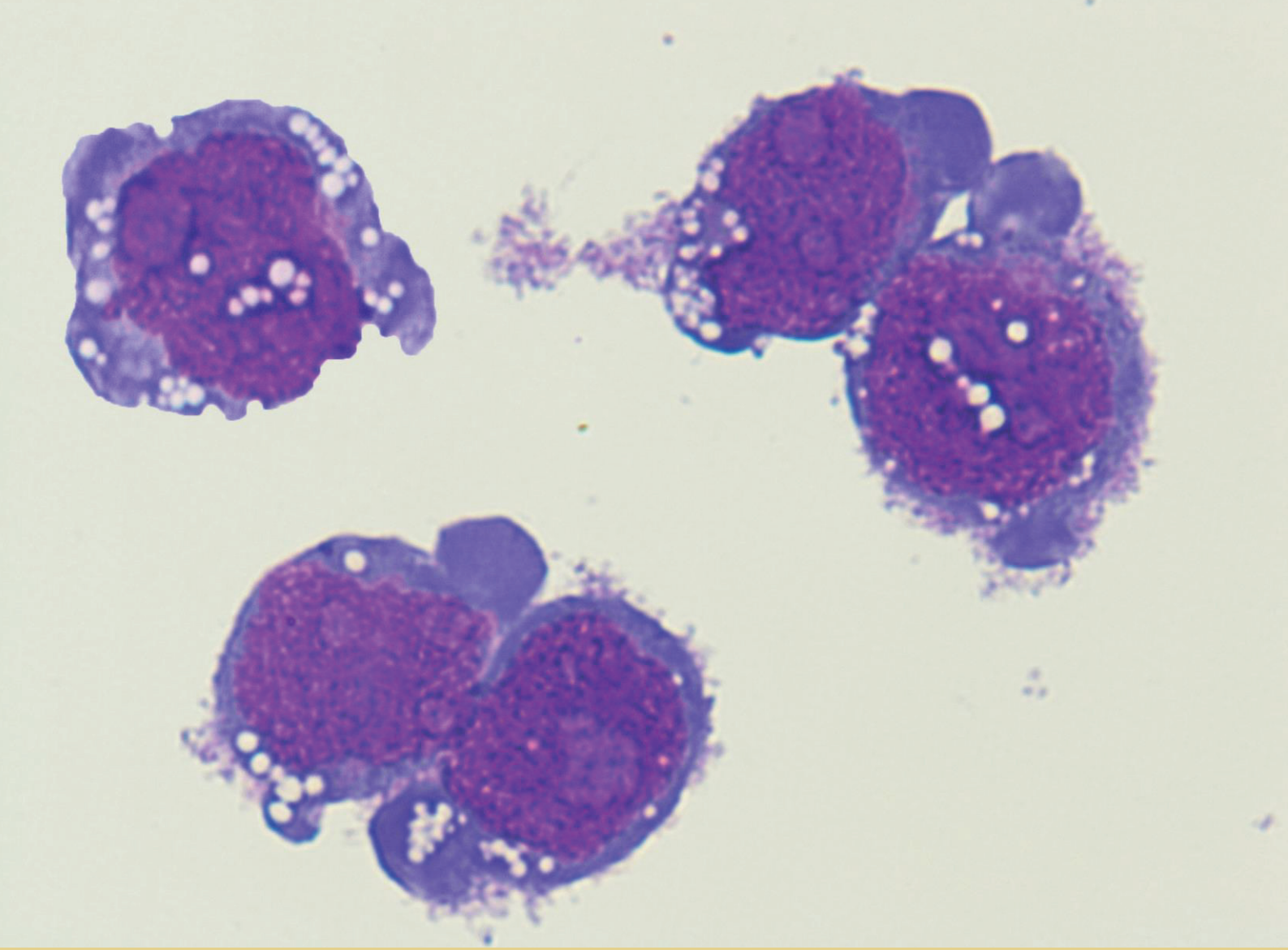

Joana Filipa Belo Penetra Neves

Cytotoxic effects of Parthenolide on lymphoid malignancies – an *in vitro* study

Dissertação de Mestrado em Biologia Celular e Molecular, orientada pela Professora Doutora Ana Bela Sarmento Antunes da Cruz Ribeiro e pela Professora Doutora Maria Carmen Martins de Alpoim e apresentada à Faculdade de Ciências e Tecnologias da Universidade de Coimbra

Setembro 2017

· U C ·

UNIVERSIDADE DE COIMBRA

Joana Filipa Belo Penetra Neves

Cytotoxic effects of Parthenolide on lymphoid malignancies – an *in vitro* study

Dissertação de Mestrado em Biologia Celular e Molecular, orientada pela Professora Doutora Ana Bela Sarmento Antunes da Cruz Ribeiro e pela Professora Doutora Maria Carmen Martins de Alpoim e apresentada à Faculdade de Ciências e Tecnologias da Universidade de Coimbra

Setembro 2017

UNIVERSIDADE DE COIMBRA

Table of contents

Table of contents

List of Figures

List of Tables

Acknowledgments

Acknowledgments

A master's thesis is an individual work, but it would never have been possible without the guidance, collaboration and support of some people to whom I would like to express my acknowledgements:

To Professor Ana Bela Sarmento Ribeiro for the guidance in this project, the support and advice, but especially for the trust. To Professor Maria Carmen Alpoim for the advice and availability throughout the master's degree.

To doctor Ana Cristina Gonçalves for the support and commitment, and for the teachings and criticism, which steered me in the right direction whenever she thought I needed it.

To doctor Raquel Alves and master Joana Jorge for the help, motivation, professional and personal advice, and, most of all, for the demonstrated patience.

To Bárbara, Beatriz, Catarina, and several other students that integrated the Laboratory of Oncobiology and Hematology (LOH) for the companionship and mutual aid that were vital throughout this year.

To the Oncology Service of Figueira da Foz's District Hospital and especially the nurse Ana Belo, for the friendship and support, for letting me know the reality of the oncological patient and the several professionals who work daily in order not only to perform the appropriate therapy, but also to give encouragement, to listen, to cherish, and to dignify those who have a difficult time. They are an inspiration and the main reason for my interest in Oncology, leading me to accept the challenge and to give my first contribution to this relevant field.

To my family, friends, colleagues, and fellow scouts for the friendship, companionship, willingness to help, and for listening when I needed the most.

Last but not least, a very special thanks to my parents and to my brother, for providing me unconditional support and continuous encouragement. This accomplishment would not have been possible without them.

Thank you for everything

Abstract

Abstract

Despite being very heterogeneous in terms of etiology, morphology, immunophenotype, and genotype, the distinct subtypes of lymphoid neoplasms resultant from B and T cell transformation at any point during its differentiation and maturation, share a relatively low/intermediate response rate to conventional chemotherapy regimens, and are frequently associated with relapse. Therefore, new therapeutic alternatives are needed. Thus, Parthenolide (PRT), a selective inhibitor of the nuclear factor kappa-B (NF-kB) pathway, which is closely associated with cancer development and aggressiveness, seems to be a valid option for hematological cancer therapy improvement.

As such, the aim of this study was to evaluate the therapeutic potential of PRT on acute lymphoblastic leukemia (ALL) and Burkitt lymphoma (BL) *in vitro* models, characterizing the type of cell death induced as well as its molecular mechanisms.

For this purpose, one BL (RAJI cells) and five ALL (697, CEM, JURKAT, MOLT-4, and KOPN-8 cells) cell lines were incubated in absence or presence of different concentrations of PRT in single or daily administration. To indirectly evaluate the effect of this drug on cell viability, the resazurin metabolic assay was used. Cell death was analyzed by optical microscopy after smear staining according to May-Grünwald Giemsa protocol, and by flow cytometry (FC), using annexin-V/7-AAD double staining. Besides this, FC was also used to clarify the molecular mechanisms involved [quantification of some apoptotic proteins (FAS, FAS-L and caspase-3) and mitochondria membrane potential, using the JC-1 probe] as well as to evaluate PRT's effect on cell cycle, phosphorylated NF-kB (p65) levels, and oxidative stress parameters (superoxide anion, hydrogen peroxide and reduced glutathione through the DHE, $DCFH_2DA$ and mercury orange probes, respectively).

The results indicate that PRT reduced the metabolic activity in time, dose, and cell line dependent manner, being KOPN-8 cells the most sensitive. This result may be related with cell type, genetic background, and disease stage at cell line establishment (at diagnosis or after relapse). Besides this, resazurin metabolic assay also revealed that

single and daily administration schemes gave similar results, indicating that daily administration should remain a possibility as it may enable a reduction in dose related systemic toxicity.

Annexin-V/7-AAD staining demonstrated that PRT have mostly a cytotoxic effect, inducing cell death preferentially by apoptosis. These results were confirmed by optical microscopy, by the increased levels of pro-apoptotic molecules, and by the sub-G_1 peak appearance in cell cycle analysis. Although cell death through apoptosis occurred in all cell lines, the mechanisms of caspase-3 activation were distinct, being cell line dependent. Indeed, extrinsic apoptotic pathway activation through FAS/FAS-L interaction was involved in all cell lines except in CEM and JURKAT. On the other hand, disruption of mitochondria membrane potential by deleterious levels of reactive oxygen species and intrinsic apoptotic pathway activation were also observed, even though to a different extent, in all cell lines.

Besides this, PRT, as revealed by FC, affected cell cycle progression particularly in JURKAT and MOLT-4 cells, where a cell cycle arrest in G_1 and G_2/M was evident.

Furthermore, the observed decrease in phosphorylated p65 levels evidenced the involvement of PRT in IKK inhibition, and consequently the NF-kB sequestering in the cytoplasm, preventing, thus, the transcription of the several genes regulated by the NF-kB pathways (e.g. the ones associated with apoptosis resistance).

In conclusion, these results suggest that PRT may represent a potential new therapeutic approach in lymphoid malignancies, presenting an important role in the regulation of a cell signaling pathway that is tightly related with control of cell growth and death. However, therapeutic efficacy may depend on cell type and genetic characteristics of the neoplasm.

Keywords:

Acute lymphoblastic leukemia; Burkitt lymphoma; apoptosis; NF-kB; oxidative stress

Resumo

A desregulação da produção de linfócitos B e T por aumento da proliferação, bloqueio da diferenciação e/ou resistência à apoptose, pode levar ao aparecimento de diversas neoplasias linfoides. Contudo, sendo muito heterogéneas em termos de etiologia, imunofenótipo e genótipo, estas partilham uma resposta relativamente baixa/intermédia aos esquemas de quimioterapia convencionais, estando frequentemente associadas a recaída. Como tal, a necessidade de novas estratégias terapêuticas implica o estudo do potencial de novos fármacos. O Partenolide (PRT), sendo um inibidor seletivo da via do fator nuclear kappa-B (NF-kB), intimamente associada ao desenvolvimento e agressividade tumoral, poderá ser uma opção válida no tratamento do cancro, nomeadamente de neoplasias hematológicas.

Como tal, o objetivo deste estudo consistiu na avaliação do potencial terapêutico do PRT em modelos *in vitro* de neoplasias linfoides, nomeadamente de leucemia linfoblástica aguda (LLA) e linfoma de Burkitt (LB), caracterizando-se o tipo de morte celular induzida e os mecanismos moleculares envolvidos.

Para este propósito, uma linha celular de LB (as células RAJI) e cinco linhas celulares representativas de diferentes subtipos de LLA (as células 697, CEM, JURKAT, MOLT-4 e KOPN-8) foram incubadas na ausência ou presença de diferentes concentrações de PRT em administração única ou fracionada. Para se avaliar, indiretamente, o efeito deste fármaco na viabilidade celular recorreu-se ao ensaio metabólico com resazurina. Quanto ao tipo de morte celular induzida, esta foi analisada por microscopia ótica, após coloração segundo o protocolo May-Grünwald Giemsa, e por citometria de fluxo (CF), utilizando a dupla coloração com anexina-V e 7-AAD.

A CF foi ainda utilizada para esclarecer os mecanismos moleculares envolvidos [avaliação dos níveis de algumas proteínas apoptóticas (FAS, FAS-L e caspase-3) e da alteração do potencial de membrana mitocondrial, recorrendo à sonda JC-1], bem como para avaliar o efeito do PRT no ciclo celular, nos níveis da forma ativa do NF-kB e nos níveis de stresse oxidativo (quantificação dos níveis de superóxido, peróxidos e

glutationa reduzida através da utilização das sondas DHE, $DCFH_2DA$ e alaranjado de mercúrio, respetivamente).

Os resultados obtidos indicaram que o PRT reduzia a atividade metabólica de forma dependente do tempo de incubação, da dose administrada e da linha celular, sendo as células KOPN-8 as mais sensíveis. Estes resultados podem estar relacionados com o tipo de célula, o genótipo e o estádio da patologia aquando do estabelecimento das linhas celulares (ao diagnóstico ou após recaída). Além disso, o ensaio metabólico com resazurina também evidenciou que a administração diária de PRT não induziu diferenças significativas na atividade metabólica celular, em comparação com o esquema de administração única, indicando que um esquema de administração fracionada pode ser uma possibilidade terapêutica, uma vez que permite uma redução das complicações associadas à toxicidade da dose administrada.

A marcação com anexina-V e 7-AAD demonstrou que o PRT tem principalmente um efeito citotóxico, induzindo morte celular preferencialmente por apoptose, o que foi confirmado por microscopia ótica, pelo aumento dos níveis de proteínas pró-apoptóticas e pela deteção do pico sub-G_1 na análise do ciclo celular. Embora a morte celular por apoptose tivesse ocorrido em todas as linhas celulares estudadas, os mecanismos de ativação da caspase-3 foram distintos. Na verdade, a diminuição do potencial de membrana mitocondrial (causa ou consequência dos níveis deletérios de espécies reativas de oxigénio) e a consequente ativação da via intrínseca da apoptose esteve presente, principalmente, nas linhas de LLA onde os resultados foram estatisticamente significativos. Por outro lado, a ativação da via extrínseca da apoptose através da interação entre a molécula FAS e o seu ligando esteve significativamente envolvida na indução de morte celular nas linhas 697 e MOLT-4.

Quanto ao efeito citostático, a análise do ciclo celular evidenciou que a progressão do mesmo não foi igualmente afetada em todas as linhas celulares, sendo as células JURKAT e MOLT-4 as únicas em que o bloqueio do ciclo celular nas fases G_1 e G_2/M foi evidente.

Para além disso, a redução nos níveis da proteína p65 fosforilada sugeriu o envolvimento do PRT na inibição da cinase IKKβ, permitindo o sequestro do NF-kB no

citoplasma e prevenindo, consequentemente, a transcrição dos vários genes que este fator regula (como vários genes associados à resistência à apoptose).

Em conclusão, estes resultados sugerem que o PRT pode representar uma potencial abordagem terapêutica em neoplasias linfoides, apresentando um papel importante na regulação de uma via de sinalização celular fortemente relacionada com o controlo do crescimento e da morte celular. No entanto, a eficácia terapêutica pode depender do tipo celular e das características genéticas da neoplasia.

Palavras-chave:

Leucemia linfoblástica aguda; linfoma de Burkitt; apoptose; NF-kB; stresse oxidativo

Abbreviations

Abbreviations

7-AAD – 7-Amino Actinomycin D

A – Aggregate

ABC – ATP-binding cassette

ABL – Abelson leukemia

AG – Antigen

ALK – Anaplastic lymphoma kinase

ALL – Acute lymphoblastic leukemia

AML1 – Acute myeloid leukemia 1

ARID5B – AT-rich interaction domain 5B

ATCC – American Type Culture Collection

ATG – Autophagy-related protein

ATP – Adenosine tri-phosphate

B-ALL – B-cell ALL

BAFFR – B cell activating factor receptor

BAK – BCL-2 homologous antagonist/killer

BAX – BCL-2-associated X protein

BCR – Breakpoint cluster region

BID – BH3 interacting-domain death agonist

BL – Burkitt lymphoma

BCL – B cell lymphoma

BCL-xL – B cell lymphoma-extra large

c-ALL – common-ALL

$CaCl_2$ – Calcium chloride

CCND3 – Cyclin D3 gene

CD – Cluster of differentiation

CDK – Cyclin-dependent kinase

CDKN2A – Cyclin-dependent kinase inhibitor 2A

CEBPE – CCAAT/enhancer binding protein epsilon

CF – *Citometria de fluxo*

cFLIP – FLICE inhibitory protein

cIAP – Cellular inhibitor of apoptosis

CLPs – Common lymphoid progenitors

CMP – Common myeloid progenitor

CO_2 – Carbon dioxide

COX2 – Cyclooxygenase-2

CTL – Control

DCF – 2',7'-dichlorofluorescein

$DCFH_2$ – 2',7'-dichlorodihydrofluorescein

$DCFH_2DA$ – 2',7'-dichlorodihydrofluorescein diacetate

DHE – Dihydroethidium

DISC – Death-inducing signaling complex

DLBCL – Diffuse large B cell lymphoma

DMSO – Dimethyl sulfoxide

DNA – Deoxyribonucleic acid

DSMZ – German Collection of Microorganisms and Cell Cultures

EBF – Early B-cell factor 1

eBL – Endemic BL

EBV – Epstein-Barr virus

ELAM-1 – Endothelial adhesion molecule 1

ETV6 – ETS variant 6

FADD – FAS-associated death domain

FADH – Flavin adenine dinucleotide hydrogen

FAS – FAS cell surface death receptor

FAS-L – FAS ligand

FBS – Fetal Bovine Serum

FC – Flow cytometry

FDC – Follicular dendritic cell

FMNH – Flavin mononucleotide hydrogen

GCLC – Glutamate-cysteine ligase catalytic subunit

gp – Glycoprotein

GPX1 – Glutathione peroxidase-1

GSH – Reduced glutathione

H_2O_2 – Hydrogen peroxide

HEPES – 4-(2-hydroxyethyl)-1-piperazineethanesulfonic acid

HHV-8 – Human herpes virus-8

HIV – Human immunodeficiency virus

HLA-DR – Human leukocyte antigen-D related

HOX11 – Homeobox 11 gene

HSCs – Hematopoietic stem cells

IAPs – Inhibitor of apoptosis proteins

IC_{50} – Half maximal inhibitory concentration

ICAM-1 – Intercellular adhesion molecule 1

ID3 – Inhibitor of DNA binding 3

Ig – Immunoglobulin

IGH – Immunoglobulin heavy locus

IkB – Inhibitor kappa B

IKK – Inhibitor kappa B kinase

IKZF1 – IKAROS family zinc finger 1

IL – Interleukin

iNOS – Inducible nitric oxide synthase

JC-1 – 5,5',6,6'-tetrachloro-1,1',3,3'-tetraethlybenzimidazolcarbocyanine iodide

JNK – c-Jun NH2-terminal kinase

LB – *Linfoma de Burkitt*

LC3 – Microtubule-associated protein 1A/1B-light chain 3

LLA – *Leucemia linfoblástica aguda*

LPS – Lipopolysaccharide

M – Monomer

MALT – Mucosa-associated lymphoid tissue

MDC – Monodansylcadaverine

MDR1 – Multidrug resistance gene

Mercury orange – 1-(4-chloromercuriophenylazo)-2-naphthol

MFI – Mean fluorescence intensity

miRNA - microRNA

miRS – microRNAs

MLL – Mixed lineage leukemia

MMP-9 – Matrix metalloproteinase-9

MnSOD – Mn superoxide dismutase

MPPs – Multipotent progenitors

mTORC1 – Mammalian target of rapamycin complex 1

MUM1 – Multiple myeloma 1

NaCl – Sodium chloride

NADH – Nicotinamide adenine dinucleotide hydrogen

NADPH – Nicotinamide adenine dinucleotide phosphate hydrogen

$NaHCO_3$ – Sodium bicarbonate

NBD – NEMO-binding domain

NEMO – Nuclear factor essential modulator

NF-kB – Nuclear factor kappa B

NHL – Non-Hodgkin Lymphoma

NIK – NF-kB-inducing kinase

NK – Natural killer

NOTCH1 – Notch homolog 1

$O_2^{\bullet-}$ – Superoxide anion

P-gp – P-glycoprotein

PAX5 – Paired box 5

PBS – Phosphate-buffered saline

PBX1 – PBX homeobox 1

PI – Propidium iodide

pre-B – Precursor B

pro-B – Progenitor B

PRT – Parthenolide / *Partenolide*

PS – Phosphatidylserine

Rb – Retinoblastoma

RNA – Ribonucleic acid

RNase – Ribonuclease

RNAi – RNA interference

RNS – Reactive nitrogen species

ROS – Reactive oxygen species

RPMI 1640 – Roswell Park Memorial Institute 1640 medium

RUNX1 – Runt related transcription factor 1

sBL – Sporadic BL

STAT3 – Signal transducer and activator of transcription 3

T-ALL – T-cell ALL

TAL1 – TAL bHLH transcription factor 1

TCF3 – Transcription factor 3

TCR – T-cell receptor

TdT – Terminal deoxynucleotidyl transferase

TFH – T-follicular helper

TIRAP – Toll-interleukin-1 receptor domain-containing adapter protein

TNF – Tumor necrosis factor

TNFR – Tumor necrosis factor receptor

TP53 – Tumor protein 53

TRAF – TNF receptor-associated factor

TRAIL-R – TNF-related apoptosis-inducing ligand receptor

VCAM-1 – Vascular cell adhesion molecule 1

VEGF – Vascular endothelial growth factor

WHO – World Health Organization

XIAP – X chromosome linked inhibitor of apoptosis

Introduction

1. Introduction

1.1. Hematopoietic System

In the blood, one of the most regenerative and plastic tissues, there is a dynamic equilibrium between cell proliferation, differentiation and death. Indeed, as mature blood cells are predominantly short-lived, a common hematopoietic progenitor must continuously reconstitute and replenish the different blood cell populations[1–9]. These hematopoietic stem cells (HSCs) are defined by their ability to self-renew, maintaining the pool of pluripotent cells, and to give rise to immature committed progenitors. These cells, through an ordered and sequential activation of a series of transcription factors[2,6–11], become more restricted in their developmental potential to myeloid and lymphoid lineages, producing the differentiated functional blood cells [myeloid cells – red blood cells, platelets, monocytes/macrophages, neutrophils, eosinophils and basophils; and lymphoid cells – B, T and natural killer (NK) cells][1–13] (Figure 1).

1.2 Lymphopoiesis

Lymphopoiesis is the process by which cellular components of the immune system are produced. In this process, HSCs are committed to differentiate into multipotent progenitors (MPPs) by progressively upregulated lymphoid lineage-specific cell-surface markers [e.g. interleukin-7 (IL-7)] and transcription factors (e.g. IKAROS and PU.1), which contribute to the loss of their potential to become myeloid precursors and to develop into common lymphoid progenitors (CLPs)[1,12]. Then, these precursors can give rise to B-cell or NK/T cell progenitors[12].

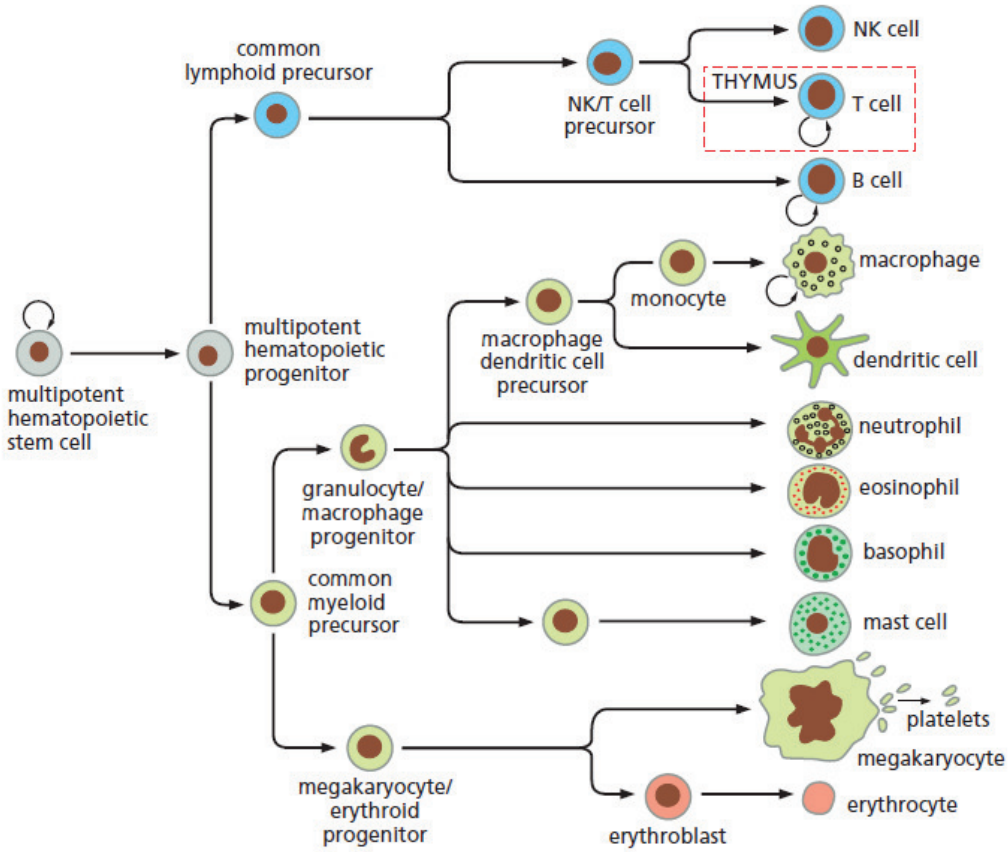

Figure 1 – Schematic representation of hematopoiesis. Hematopoietic stem cells (HSCs) self-renew and originate multipotent progenitors (MPPs), which in turn differentiate into a common lymphoid precursor (CLP) or a common myeloid progenitor (CMP). These cells will give rise to more differentiated progenitors, culminating in matured and differentiated blood cells. From *Alberts et al 2014*[169]

1.2.1 B cell development

The initiation of early B cell development is controlled by a hierarchical regulatory network of transcription factors, including PU.1, E2A, early B-cell factor 1 (EBF), and paired box 5 (PAX5), which are not only essential for B cell commitment maintenance, but also to the rearrangement of immunoglobulin variable-region genes which is a crucial process in B cell formation[6,7,14]. Therefore, early lymphoid progenitors (pre-pro-B cells) progressively mature into irreversibly committed progenitor B (pro-B) cells, precursor B (pre-B) cells, which are in the initial stages of immunoglobulin rearrangement, and finally in immature B cells[6,7, 12,14]. Then, these naïve B cells

expressing cell-surface immunoglobulin M (IgM) leave the blood marrow and are carried by the venous supply to the spleen[7, 12,14,15]. From this secondary lymphoid organ, cells can re-enter in blood and upon antigen encountering they migrate to germinal centers of lymph nodes where they initiate monoclonal expansion and go through isotype switching and somatic hypermutation, increasing the affinity of the antibodies produced. Then, these centroblasts migrate from the dark to the light zone, start expressing their antibodies and become centrocytes. The centrocytes that survive germinal center selection, which are B clones that gained mutations that confer higher affinity antibodies towards the antigen, receive a differentiation signal to exit the light zone as either memory B cells or plasmoblasts, which then migrate to the bone marrow where they mature into antibody secreting plasma cells[7,15] (Figure 2).

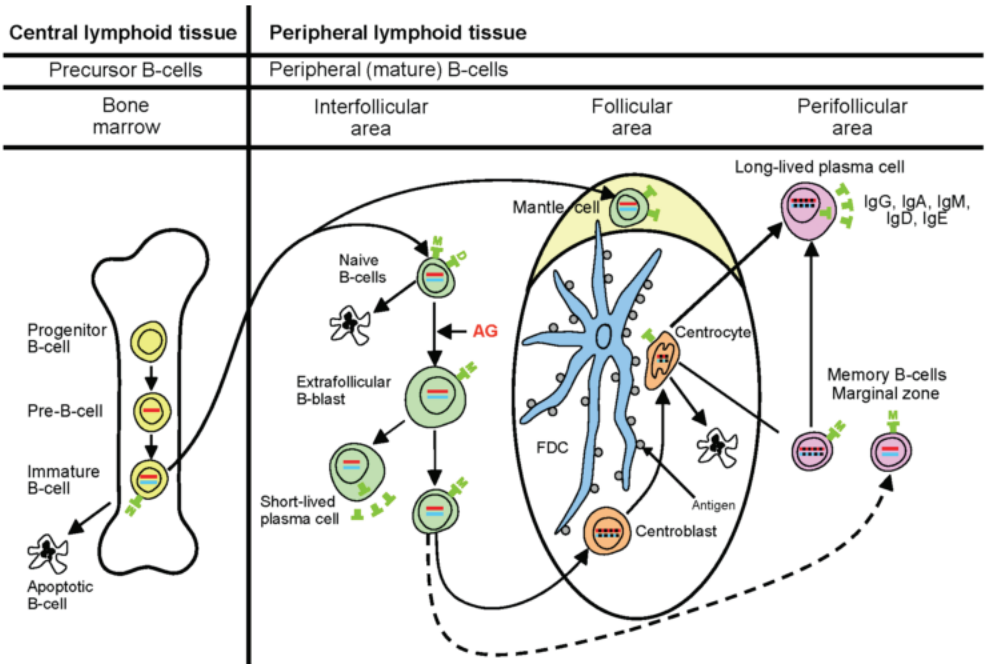

Figure 2 – Schematic representation of B cell differentiation. AG, antigen; FDC, follicular dendritic cell; Ig, immunoglobulin. Adapted from *Stewart & Wild 2014*[20]

1.2.2 T cell development

T cell development is initiated upon up-regulation of E24 and Notch homolog 1 (NOTCH1) transcription factors and consequent shift of T/NK progenitors into

committed T cell progenitors (prothymocytes) which migrate to the subcapsular region of thymic lobule where they undergo distinct maturation steps and immunological education[6,7,12]. Within the thymus, these population of subcortical thymocytes, which are cluster of differentiation 7 (CD7) and 34 (CD34) positive, but do not express CD4 or CD8 (double-negative), interact with the thymic stroma and start expressing CD2, CD3, and terminal deoxynucleotidyl transferase (TdT) genes[6,7,12]. By this stage, T-cell receptor (TCR) gene rearrangement is underway and immature thymocytes can start expressing γδ or αβ receptors, becoming γδ T cells or αβ lineage precursors, respectively[7]. Then, medullary αβ cells start to express CD4 and CD8 (double-positive stage) and are submitted to positive and negative selection[7,12]. This results in the generation of immunocompetent $CD4^+$ or $CD8^+$ T cells[6,7,12] which enter the secondary lymphoid tissue[7]. In the lymph nodes, following exposure and recognition of the antigen, there is naïve lymphocytes' expansion (T-blasts) and differentiation into effector and memory cells[12] (Figure 3).

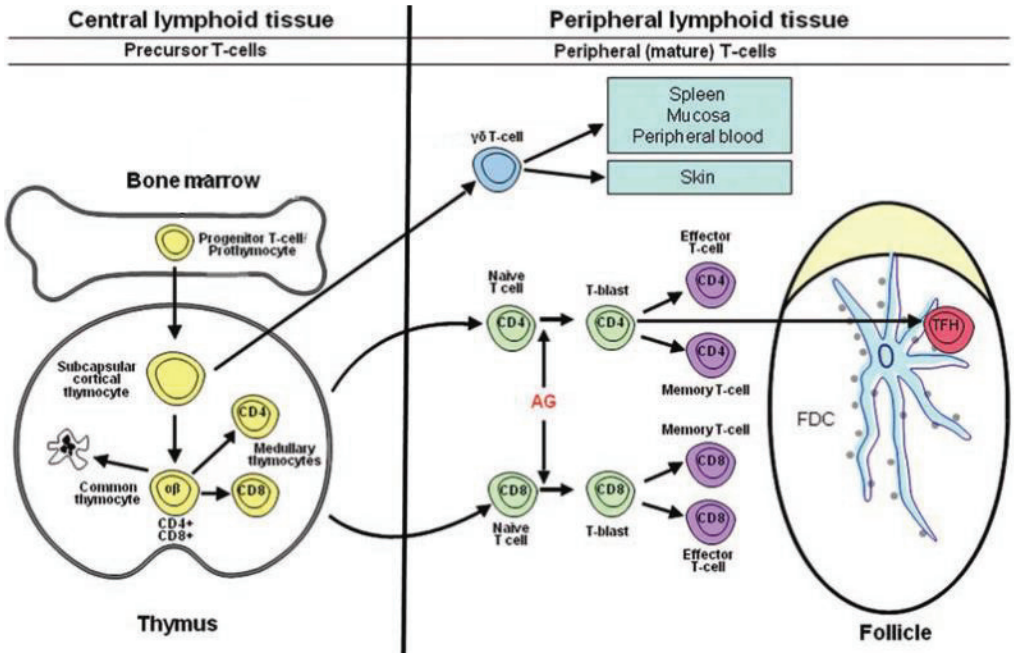

Figure 3 – Schematic representation of T cell differentiation. AG, antigen; FDC, follicular dendritic cell; TFH, T-follicular helper. Adapted from *Stewart & Wild 2014*[20]

1.3 Lymphoid malignancies

The short half-life of blood cellular components and their constant replacement and maturation make hematopoiesis very susceptible to errors' accumulation and, consequent, to the development of hematological malignancies[6,7,13]. Indeed, the disruption in differentiation and maturation of blood cells by differentiation arrest, apoptosis resistance, and/or increased proliferation can lead to stage-specific neoplasms[7, 9, 12,13,16–18]. Lymphoid malignancies are a heterogeneous group of hematological neoplasms which originate from neoplastic transformation of B, T, and NK cells' at any stage of differentiation and maturation[12,16,17]. The current classification of these wide group of hematological malignancies considers the maturity of the cell lineage affected, the clinical progression of the disease and the presence of genetic alterations, mainly mutations and translocations (Table 1)[12].

1.4 Acute lymphoblastic leukemia

Acute lymphoblastic leukemia (ALL) is an aggressive neoplasm characterized mainly by proliferation and accumulation of lymphoid progenitors. These lymphoblasts committed to become B [B-cell ALL (B-ALL)] or T [T-cell ALL (T-ALL)] cells accumulate in bone marrow (and/or thymus in the case of T-ALL)[6,7, 12,19–21] and result in the suppression of hematopoiesis by competition with normal hematopoietic cells, leading to anemia, thrombocytopenia, and neutropenia. These undifferentiated blasts can disseminate through bloodstream, infiltrating other organs and tissues such as brain, liver, spleen, lymph nodes, and testis[6,7, 12,22,23].

This disease can occur at any age[12,24], having a bimodal distribution with 60% of cases being diagnosed in patients younger than 20 years of age[24,25] (the first incidence peak occurs at 2 to 5 years[19,26–28]) and registering a second peak around the fifth decade of life[6,25]. It accounts for approximately 80% of childhood leukemias[7,25] and 20% of leukemia diagnosis in adults[25]. Regarding the cells affected, B cell lineage leukemia is more incident, being B-ALL diagnosed in 85% of cases[6].

Table 1 – World Health Organization (WHO) classification of lymphoid neoplasms regarding B and T cell lineages

PRECURSOR LYMPHOID NEOPLASMS - B lymphoblastic leukemia/lymphoma - T lymphoblastic leukemia/lymphoma **MATURE B CELL NEOPLASMS** - Chronic lymphocytic leukemia/small lymphocytic lymphoma - B-cell prolymphocytic leukemia - Splenic B-cell marginal zone lymphoma - Lymphoplasmacytic lymphoma - Heavy-chain diseases - Plasma cell neoplasms - Extranodal marginal zone lymphoma of mucosa-associated lymphoid tissue (MALT lymphoma) - Nodal marginal zone lymphoma - Follicular lymphoma - Primary cutaneous follicle center lymphoma - Mantle cell lymphoma - Diffuse large B cell lymphoma (DLBCL) - DLBCL associated with chronic inflammation - Lymphomatoid granulomatosis - Primary mediastinal (thymic) large B cell lymphoma - Intravascular large B cell lymphoma - Anaplastic lymphoma kinase (ALK) positive large B cell lymphoma - Plasmatic lymphoma - Large B cell lymphoma arising in human herpesvirus 8 (HHV-8) associated multicentric Castleman disease	- Primary effusion lymphoma - Burkitt lymphoma - B cell lymphoma, unclassifiable, with features intermediate between DLBCL and classical Hodgkin lymphoma **MATURE T CELL NEOPLASMS** - T cell prolymphocytic leukemia - T cell large granular lymphocytic leukemia - Epstein Barr virus (EBV) positive T cell lymphoproliferative disorders of childhood - Adult T cell leukemia/lymphoma - Extranodal T cell lymphoma - Enteropathy-associated T cell lymphoma - Hepatosplenic T cell lymphoma - Subcutaneous panniculitis-like T cell lymphoma - Mycosis fungoides - Sézary syndrome - Primary cutaneous CD30-positive T cell lymphoproliferative disorders - Primary cutaneous peripheral T cell lymphoma - Peripheral T cell lymphoma - Angioimmunoblastic T cell lymphoma - Anaplastic large cell lymphoma, ALK-positive - Anaplastic large cell lymphoma, ALK-negative **HODGKIN LYMPHOMA** - Nodular lymphocyte predominant Hodgkin lymphoma - Classical Hodgkin lymphoma

Adapted from *Kaushansky et al 2016*[12]

1.4.1 Etiology and pathogenesis

Despite the fact that the precise pathogenic events leading to this disease are still unknown[7, 12,26,27], ALL is thought to arise from interactions between environmental factors and host genetic (inherited) susceptibility[7, 12, 19,24]. Indeed, several genetic

syndromes, such as Down[26], Bloom, and Nijmegen breakage syndrome, neurofibromatosis type I, ataxia-telangiectasia[19,27], and polymorphic variants/mutations in several genes [AT-rich interaction domain 5B (*ARID5B*), CCAAT/enhancer binding protein epsilon (*CEBPE*), *GATA3*, IKAROS family zinc finger 1 (*IKZF1*), *PAX5*, ETS variant 6 (*ETV6*), cyclin-dependent kinase inhibitor 2A (*CDKN2A*), etc.] as well as exposure to radiation and certain chemicals have been implicated in the induction of ALL[7, 12, 19, 24,26,27]. Besides this, childhood ALL is also thought to result from an abnormal response to common infections which led to the development of genetic errors due to the overproliferation of immune cells[7].

The advances in technology and the emergence of high-resolution profiling of genetic alterations made possible a better understanding of the general mechanisms underlying the induction of ALL both in children and in adults[24,29]. The initiation and progression of ALL is driven by successive heterogenic mutations that alter cellular functions[12,19], such as aberrant expression of proto-oncogenes, through chromosomal translocations, which may affect the immunoglobulin or TCR genes[19,27], resulting in chimeric[23] fusion genes encoding active kinases and altered transcription factors, or by hyper- or hypodiploidy[29], and point mutations or deletions[23] (Figure 4). As a consequence, these alterations maintain or promote an enhance unlimited ability to self-renewal, lead to uncontrolled cell proliferation, block differentiation, and increase resistance to apoptosis[12,29].

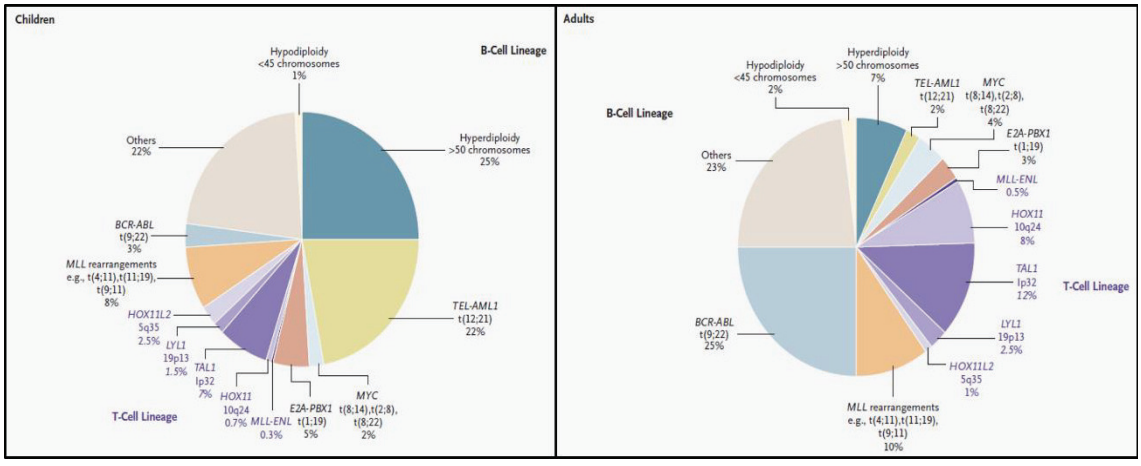

Figure 4 – Specific genotypes of acute lymphoblastic leukemia (ALL) in children and adults. Within B-ALL there are several specific genetic alterations (indicated in black) which comprise abnormalities in the number of chromosomes [hyper- (>50) or hypodiploidy (<44)] and chromosomal translocations, such as *ETV6-RUNX1* [t(12;21)(p13;q22)], *BCR-ABL1* [t(9;22)(q34;q11.2)], and *MLL* [t(v;11q23)] translocations, that generate fusion genes

encoding transcription factors or active kinases. Regarding T-ALL (indicated in purple), some of the genes deregulated include *TAL1* and *HOX11*. Besides that, the deletion of *CDKN2A/B* genes and the activation of NOTCH1 can also be present[6,7,12]. RUNX1, runt related transcription factor 1; BCR, breakpoint cluster region; ABL, Abelson leukemia; MLL, mixed lineage leukemia; TAL1, TAL bHLH transcription factor 1; HOX11, homeobox gene 11 gene. From *Pui, Relling and Downing 2004*[29]

1.4.2 Classification

An important feature of ALL is the typical presence of blasts, at least 20%, in the bone marrow and/or peripheral blood. Leukemic blast cells are currently characterized by morphology (L1 – scant cytoplasm without granules; L2 – large and heterogeneous cells with abundant cytoplasm; L3 – deeply basophilic with cytoplasmic vacuolation), cytogenetics (Table 2), and immunological tests[6,12].

Table 2 – WHO classification of acute lymphoblastic leukemia

SUBTYPE	EVENT FREE-SURVIVAL (%)	
B-cell acute lymphoblastic leukemia	**Children**	**Adults**
B-ALL with recurrent genetic abnormalities		
B-ALL with t(9;22)(q34;q11.2) *BCR-ABL1*	80-90 at 3 years	~ 60 at 1 year
B-ALL with t(v;11q23); *MLL* re-arranged		
B-ALL with t(12;21)(p13;q22) *TEL-AML1* (*ETV6-RUNX1*)	90-95 at 5 years	
B-ALL with hyperdiploidy (>50)	80-90 at 5 years	30-50 at 5 years
B-ALL with hypodiploidy (<44)	30-40 at 3 years	10-20 at 3 years
B-ALL with t(5;14)(q31;q32) *IL3-IGH*		
B-ALL with t(1;19)(q23;p13.3) *TCF3-PBX1*	82-90 at 5 years	20-40 at 3 years
T-cell acute lymphoblastic leukemia	**Children**	**Adults**
NOTCH1 mutations	90 at 5 years	50 at 4 years
HOX11 overexpression	90 at 5 years	80 at 3 years

AML1, acute myeloid leukemia 1; IGH, immunoglobulin heavy locus; TCF3, transcription factor 3; PBX1, PBX homeobox 1.

Adapted from *Hoffbrand & Moss 2016*[6], *Hoffbrand et al 2016*[7] and *Kaushansky et al 2016*[12]

As such, according to immunology methods, B-ALL can be subdivided into: pro-B-ALL, common ALL (c-ALL), and pre-B-ALL. In pro-B-ALL the leukemic blasts resemble normal B cell precursors that always express CD19 and, in most cases, have TdT, cytoplasmic CD79a, and surface and cytoplasmic CD22. CD10 and surface and cytoplasmic immunoglobulins are not expressed. c-ALL and pre-B-ALL are very similar, being the cytoplasmic accumulation of immunoglobulin μ heavy chains with no surface immunoglobulins (pre-B-ALL) the only difference between the two. Therefore, both subtypes express CD19, CD22, CD79a, CD10, and TdT, and only two-thirds express CD34[7].

On the other hand, T-ALL, according to the stage of intrathymic differentiation, can be classified into: early T-precursor ALL, positive for CD7, and cytoplasmic CD3 but negative for further differentiation markers; thymic/cortical T-ALL, with expression of CD1a, CD4, CD8, and cytoplasmic CD3; and mature T-ALL, which express surface CD3, either CD4 or CD8, and is negative for CD1a. Besides this, all subtypes are TdT positive and express the antigen glycoprotein (gp) 40 (CD7)[7].

1.4.3 Treatment and Prognosis

In general, ALL treatment comprises 4 phases – induction (to restore normal hematopoiesis), intensification (to prevent recurrence and decrease the minimal residual disease), consolidation, and maintenance[6]. However, since ALL is a heterogeneous neoplasm with many distinct subtypes, the approach to therapy is not uniform. Therefore, treatment protocols are adjusted and planned according to the age, gender, white cell count, cytogenetics, immunophenotype, and presence of central nervous system disease, which are important prognostic factors (Table 2 and 3)[6,7,12].

For this reason, the therapeutic regimens selected to treat children are slightly distinct from the ones administered to adults, being the levels of cytotoxicity the main difference. Although both (induction and consolation) regimens include a glucocorticoid element (prednisone, prednisolone or dexamethasone), vincristine, L-asparaginase, and cyclophosphamide, anthracyclines (daunorubicin or doxorubicin) are only used to treat

adults and children with a very poor prognosis (daunorubicin)[7,12]. Regarding the maintenance phase, both groups frequently receive methotrexate and 6-mercaptopurine (also cytarabine in children) with vincristine and steroid pulses[7,12]. Besides this, patients with *BCR-ABL1* rearrangement can also be treated with selective tyrosine kinase inhibitors (imatinib and dasatinib)[7].

With all this therapeutic options and with the emergence of adapting therapy to the present genetic alterations, improvements in supportive care, and amelioration and development of new chemotherapy drugs, more than 85%[30] of children and 40% of adults can expect long-term leukemia-free survival and probable cure[6,23]. However, the regimens administered can be associated with acquired therapy resistance (10% of children suffer early relapse[7]; in adults the overall frequency of relapse is 50%[19]) and are often related with severe acute toxicities and long-term side effects, including cardiotoxicity, endocrinopathy, and the development of secondary tumors later in life, which decrease the quality of life of the patients[23,24].

Table 3 – Prognostic factors commonly used to stratify ALL's therapy

FACTOR	POOR	GOOD
Age	Adult (or infant < 1 year)	Child
Gender	Male	Female
White cell count	High	Low
Cytogenetics	≥5 chromosomal abnormalities Hypodiploidy *BCR-ABL1* and *MLL* rearrangements	Normal or hyperdyploidy *ETV6* rearrangement
Immunophenotype	T-ALL	B-ALL
CNS disease	Present	Absent

Adapted from *Hoffbrand & Moss 2016*[6] and *Hoffbrand et al 2016*[7]

1.5 Burkitt lymphoma

Burkitt lymphoma (BL) is a highly aggressive lymphoma[6,7, 12, 16,31–35] derived from a germinal center B cell[6,7, 12,32] [positive for: B cell lymphoma-6 (BCL6), CD10, CD19, CD20, CD22, CD38, CD79a, and surface immunoglobulin; and negative for: CD5, CD23, CD30, CD43, CD138, multiple myeloma 1 (MUM1), and cytoplasmic immunoglobulin[6,7,12]] that proliferate at a high mitotic rate[6,7, 16,31–36]. This non-Hodgkin lymphoma (NHL)[6,7, 16, 31,34,35] is very common in younger people, accounting for 30[16] to 50% of childhood lymphomas[35], and is a rare disease in adults[12, 16,35], making up less than 1% of NHL in the United States[16]. The median age in the adult group is 30 years[35].

1.5.1 Clinical variants

Based on clinical and epidemiological characteristics, BL is subdivided into three distinct categories: endemic BL (eBL), sporadic BL (sBL), and immunodeficiency-associated BL[6,7, 12, 16, 20, 31,32,34–37].

Endemic BL usually occurs in equatorial Africa[12, 20, 31, 35,37] and Papua New Guinea[7, 32, 34,36] with a peak age incidence at 4 to 7 years[7, 12,31]. Epstein-Barr virus (EBV) infection[6, 9, 20, 31,32,35–37] is present in about 95%[7, 12,34] of patients and an association with malaria and certain other environmental factors can also be established[6,12]. Clinically, eBL presents as tumors affecting the jaw and facial bones[6,7, 12,34,35] and can spread to extranodal sites, such as the marrow and the meninges[7,12].

Sporadic BL is encountered outside endemic African regions[6,7, 12,32], mainly in Western Europe and the United States[16,35], where it accounts for 1 to 2% of NHL[12] and has a median age at diagnosis of 30 years[12, 31,35]. EBV is positive in 20% of sBL cases[6, 12,32] and most patients present with peripheral lymphadenopathy or an intra-abdominal mass[7,16] (in the gut, mainly the terminal ileum), and in the upper respiratory tract[34,35].

Immunodeficiency-associated BL occurs in immunosuppressed patients positive for human immunodeficiency virus (HIV)[12, 16, 31,32,35,36] and can be related to EBV in

approximately 30%[12,36] of cases. Clinically, there is frequent nodal[12] and bone marrow localization[35].

Finally, the non-endemic forms of BL have propensity to metastasize to the central nervous system[12,16], kidneys, gonads, breast, and marrow[12] (sBL).

1.5.2 Etiology and pathogenesis

Despite the fact that precise pathogenic events leading to this disease are still unknown[7, 12,26,27], BL has been related to EBV and *Plasmodium falciparum* (malaria) infections[6,12] and some molecular mechanisms have been proposed to explain this apparent connection. One of these theories postulates that EBV initiates a polyclonal proliferation of B cells, which is further stimulated by malaria and other infections, leading to deregulated cytidine deaminase activation and consequent predisposition to genetic alterations acquisition and neoplastic transformation[12].

Therefore, the previous mechanism can be one of the explanations, at least in the case of eBL, for constitutive activation of the *MYC* proto-oncogene through micro ribonucleic acid [mi(RNA)] deregulation (less than 10% of sBL[34]) or, in most cases, immunoglobulin translocation[12, 16, 20,31–39], which is dependent on the enzymatic activity of cytidine deaminase during class-switch reaction and somatic hypermutation[12,34]. Thus, 80%[34] of all BLs show a translocation between the long arm of chromosome 8 (the site of the *MYC* gene) and the immunoglobulin[20] heavy-chain region on chromosome 14 [t(8:14)][6,7, 32,36]. Other cases of BLs have translocations between chromosome 8 and light-chain locus on chromosome 2 [t(8:2)] or on chromosome 22 [t(8:22)][6,7, 12, 16, 31, 34,35,39]. As a result, the synthesis of the c-MYC protein increases and allows an unregulated cellular growth and proliferation[34,39] by enabling the transcription of a plethora of genes involved in cell growth[12,39]. Besides this, c-MYC also cause metabolic reprogramming, deregulation of cell cycle control, and genetic instability[35]. Alterations at the tumor protein 53 (*TP53*) gene at chromosome 17[35], which lead to apoptosis blocking, can also be found (40% of BL cases)[7,12]. Additional chromosome abnormalities can also be present, altering the expression of other important genes such as proto-

oncogenes [cyclin-D3 gene (*CCND3*) and *TCF3*][7,12], tumor suppressor genes [inhibitor of DNA binding 3 (*ID3*)][7, 12,35], or some key players in apoptosis[32,37] that cooperate with MYC to promote proliferation, survival, and growth of B cells[7].

1.5.3 Treatment

Despite being the most rapidly progressive human tumor[16], treatment with intensive chemotherapy regimens[6,7, 12, 16, 33,35] (Table 4) lead to cure[7,12] in 70-80% of both children and young adults[16]. However, many older patients do not tolerate the conventional therapies[7, 12,32] and the immunosuppression caused by them is not a valid option in eBL treatment[32]. In addition, the presence of complications, central nervous system relapse[31] and therapy-resistant disease[12] are an important reality.

Table 4 – Therapeutic regimens available for Burkitt lymphoma treatment

REGIMEN	2-YEAR OUTCOME
Short duration / dose intensive	51% estimated survival
Short duration / dose intensive with rituximab	74% (3-year) event-free survival
CODOX-M/IVAC	64% progression-free survival
R-CODOX-M/IVAC	80% progression-free survival
Hyper-CVAD with rituximab	89% estimated survival
R-EPOCH	95% event-free survival

CODOX-M/IVAC, cyclophosphamide, doxorubicin, vincristine, methotrexate, ifosfamide, etoposide and cytarabine; **R-CODOX-M/IVAC**, CODOX-M/IVAC with rituximab; **Hyper-CVAD**, cyclophosphamide, vincristine, doxorubicin and dexamethasone; **R-EPOCH**, etoposide, vincristine and doxorubicin with rituximab, cyclophosphamide and steroids.

Adapted from *Hoffbrand & Moss 2016*[6], *Hoffbrand et al 2016*[7] and *Kaushansky et al 2016*[12]

1.6 Nuclear Factor Kappa B (NF-kB)

The transcription factor nuclear factor kappa B (NF-kB) plays an important role in T and B cell development, proliferation, and survival, controlling the expression of positive cell cycle regulators, anti-apoptotic factors, as well as inflammatory and immunoregulatory genes[40–49]. Therefore, deregulated NF-kB activation has been associated with multiple pathologies, including inflammatory diseases, immune deficiencies, diabetes, atherosclerosis, and cancer, including lymphoid malignancies[40–43,50].

1.6.1 NF-kB signaling pathways

The NF-kB family of transcription factors is composed of 5 major proteins – NF-kB1 (p50 and its precursor p105), NF-kB2 (p52 and its precursor p100), RelA (p65), RelB, and c-Rel[40–44,49–55]. These proteins form various homodimers and heterodimers[40, 42,43, 50,55] which, in unstimulated cells, are kept inactive by cytoplasmic association with inhibitor kappa B (IkB) proteins (IkBα, IkBβ, IkBγ, IkBε, p105, and p100)[40–44, 50–52,55]. The activation of NF-kB signaling by a wide variety of extracellular stimuli, such as tumor necrosis factor-alpha (TNF-α), IL-1β, growth factors, B or T cell activation, and oxidant-free radicals, occurs through two general pathways – the classical or canonical and the alternative or non-canonical – which are both based on the inducible phosphorylation of IkB by IkB kinases (IKK) and the consequent ubiquitination and degradation of these protein, allowing NF-kB activation and translocation to the nucleus[40–45, 49–53,55] (Figure 5).

1.6.1.1 Canonical NF-kB pathway

The canonical pathway of NF-kB activation can be engaged by a plethora of stimuli, such as pro-inflammatory cytokines and antigens, external signaling through B cell and

T cell receptors, and some tumor necrosis factor receptors (TNFRs)[40, 42, 49, 53,56–59]. Following this stimulation, the IKK complex [IKKα, IKKβ, and IKKγ or nuclear factor essential modulator (NEMO)] is activated and phosphorylates the inhibitory subunits of the IkB complex, leading to their polyubiquitination and proteasomal degradation, which abrogates the inhibitory association between IkB and NF-kB. Then, NF-kB dimers are able to migrate to the nucleus where they bind to deoxyribonucleic acid (DNA) regulatory elements and activate the transcription of several genes[40–42, 49–53, 55,58,59], particularly the ones involved in immune response and inflammation[42,43, 49, 53,58,59], cell proliferation, survival[40, 42,43, 47–49, 51, 53,58,59], and adhesion[40, 42, 51,58,59].

1.6.1.2 Non-canonical NF-kB pathway

The alternative NF-kB pathway is an additional signaling cascade very important in lymphoid development and B cell maturation[42,43, 49,58,59] that is only induced by a restricted set of TNFR, including CD40, the lymphotoxin β receptor and B cell activating factor receptor (BAFFR) [40, 42,58,59]. In this pathway, the activation of IKKα homodimers leads to the partial proteolysis of p100 to the active p52, which preferentially dimerizes with RelB. Then, this complex is translocated to the nucleus and acts as a transcription factor[40, 42,43, 51,58,59]. In addition, this pathway also induces p105 phosphorylation by the classical IKK complex, leading to its ubiquitination and subsequent degradation, releasing p50 homodimers that migrate to the nucleus and induce gene transcription[43]. Furthermore, activation of the alternative pathway depends on NF-kB-inducing kinase (NIK) which during unstimulated conditions is targeted for degradation by TNF receptor-associated factor 2 (TRAF2) and TRAF3 complex, as well as cellular inhibitor of apoptosis 1 or 2 (cIAP1/2), and upon stimulation leads to IKKα phosphorylation also inducing p100 partial proteolysis[40, 43,44, 49, 51–53,58].

Finally, something common to both pathways is the NF-kB promotion of IkBα synthesis that enters in the nucleus and removes NF-kB from DNA, exporting the complex back to the cytoplasm restoring the original state[40,43].

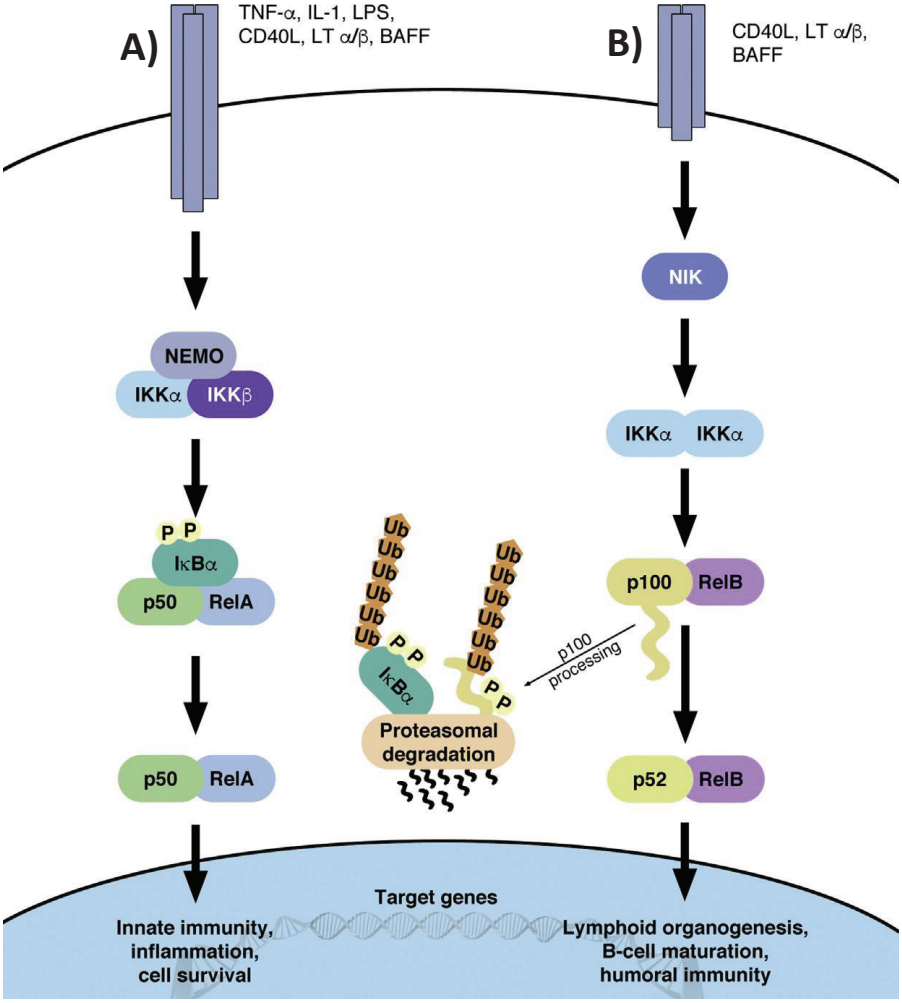

Figure 5 – Canonical (A) and non-canonical (B) NF-kB pathways. A) Activation of the canonical pathway. Activated IKK phosphorylates IkB, inducing its polyubiquitinylation and consequent proteolytic degradation by the proteasome. Then, the cytoplasmic NF-kB dimers translocate into the nucleus, where they undergo a series of posttranslational modifications and regulate the transcription of over 500 genes[42,58,59] involved in inflammation (*TNF*, *IL-1*), proliferation [c-*MYC*, *CYCLIN D*, *IL-6*, signal transducer and activator of transcription 3 (*STAT3)*, *TNF*], anti-apoptosis/survival [B cell lymphoma-2 (*BCL-2)*, B cell lymphoma-extra large (*BCL-XL)*, cellular inhibitor of apoptosis (*cIAP*), X chromosome linked inhibitor of apoptosis (*XIAP*), FLICE inhibitory protein (*cFLIP*), Mn superoxide dismutate (*MnSOD*), survivin)] immortality (*telomerase*), tumor promotion [cyclooxygenase-2 *(COX2*), inducible nitric oxide synthase (*iNOS*), matrix metalloproteinase-9(*MMP-9*)], angiogenesis [vascular endothelial growth factor (*VEGF*), *TNF*, *IL-1*, *IL-8*], and metastasis [intercellular adhesion molecule 1 (*ICAM-1*), vascular cell adhesion molecule 1 (*VCAM-1*), endothelial adhesion molecule 1 (*ELAM-1*)][42, 56–59, 147,170]. B) Activation of the non-canonical pathway. This pathway culminates in the activation of IKKα, which phosphorylate p100 inducing its partial proteolysis. Then, the resultant p52-RelB dimers translocate into the nucleus[42,58]. IKK, IkB kinase; IL, interleukin; IkB, inhibitor of NF-kB: LPS, lipopolysaccharide; TNF, tumor necrosis factor. From *Durand & Baldwin 2017*[58]

1.6.2 NF-kB and cancer

Since NF-kB is responsible for the regulation of many important biological processes, this transcription factor plays a crucial role in cancer development and aggressiveness by enhancing tumor angiogenesis, proliferation, survival, and resistance to apoptosis, as well as to chemo and radiotherapy[40,41, 43–45, 50,54,55]. Indeed, various events lead to constitutive activation of NF-kB signaling in various tumors, such as breast[56,60], colorectal[45,48], glioblastomas[60], prostate[56] and ovarian cancers[48], and certain forms of lymphoid malignancies[42,48], including Hodgkin disease[42, 45,60], NHL[42,60], multiple myeloma[49, 51–53, 56,60–62], ALL[41,56], and BL[35, 41,47,48]. Regarding the genetic and molecular alterations, overproduction of the ligands[49, 51, 53,61] and mutations in the receptors[51,61] (CD40, TNFR, BAFFR), in some members of the NF-kB family[51,61] (NF-kB1 and NF-kB2) and in NIK[49, 51,61] and its regulators[49,51] (TRAF2, TRAF3 and cIAP1/2) can be detected. All of these possible alterations in a broad range of pathologies highlight the importance of this pathway in cancer, indicating that its inhibition may be a valid therapeutic target (Figure 6). In fact, some drugs that inhibit the activation of NF-kB by inhibiting the degradation of its inhibitor in the proteasome (e.g. bortezomib in the treatment of multiple myeloma) are already used in the clinic[44,63–67].

1.6.3 Parthenolide

Parthenolide (PRT) (Figure 7) is a natural sesquiterpene lactone[45, 47, 52, 54, 62,68–76] which suppresses inflammation and shows multiple anti-tumoral and pro-apoptotic characteristics[68,69,76]. Indeed, *in vitro* treatment with PRT withdraws cells from cell cycle[69], inhibits DNA synthesis[47] and angiogenesis[77], promotes cell differentiation[45,46], and leads to cell death[70,78]. This induction of apoptosis[45, 47, 62, 68–70, 73–75,77,78] occurs through NF-kB signaling pathway inhibition[52, 58, 62, 68,69, 72,73, 75–77,79–82], oxidative stress promotion[45, 68,69, 72,73, 75,76, 79,81,82], p53 activation[46, 72,73, 76,79], BCL-2-associated X protein (BAX) and BCL-2 homologous antagonist/killer (BAK) conformational changes, as well as BH3 interacting-domain death agonist (BID) cleavage[45].

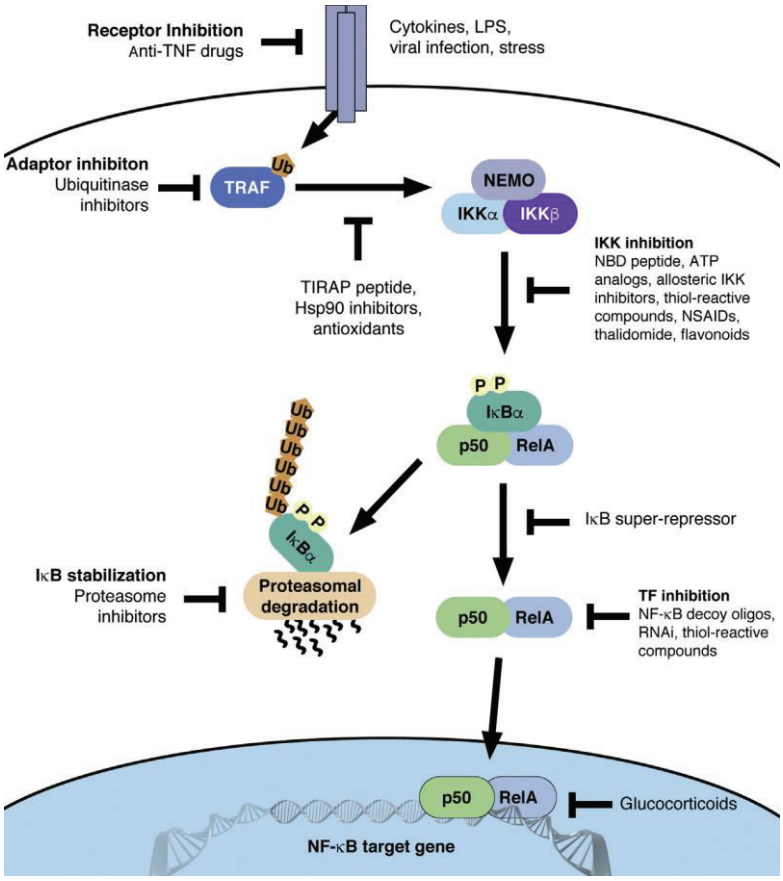

Figure 6 – NF-kB pathway inhibition. NF-kB pathways, mainly the canonical one, can be inhibited at multiple levels, leading to NF-kB suppression and proliferation inhibition, cell cycle arrest, and apoptosis[56,58]. Indeed, there are a number possible therapeutic approaches which selectively target IKK activity [Adenosine tri-phosphate (ATP) analogs[58,59], curcumin[58,171], resveratrol[171], thiol-reactive compounds[58,59], thalidomide[41,60], NEMO-binding domain (NBD) peptide], proteasome-mediated degradation of IkB (bortezomib[41,58–60], lactacystin[58]), nuclear translocation of NF-kB, DNA binding (thiol-reactive compounds[58]), and transcriptional activity of the NF-kB complex [glucocorticoids, NF-kB decoy oligos and RNA interference (RNAi)][58,60]. TIRAP, toll-interleukin-1 receptor domain-containing adapter protein. Adapted from *Durand & Baldwin 2017*[58]

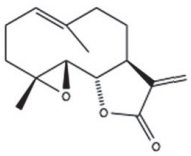

Parthenolide (PRT)

Figure 7 – Chemical structure of Parthenolide (PRT). Adapted from *Gali-Muhtasib et al 2015*[83]

1.6.3.1 Parthenolide promotes NF-kB inhibition

One important PRT effect is the potent[45,46] inhibition of NF-kB signaling through two different processes. This compound is capable of interacting with p65 subunit at the cysteine residue in its activation loop, preventing its binding to the respective regulatory region in the DNA[45,46, 54, 58, 70,80–82]. Another target of PRT is the IKK complex (forms a covalent bond with the thiol group of IKKβ's cysteine-179) which then is unable to phosphorylate and promote the proteolysis of IkB proteins. As a consequence, the NF-kB dimer is sequestered at the cytoplasm, resulting in gene expression suppression[45–47, 52, 54, 58, 68–70, 79,81,82].

Furthermore, PRT can induce cell death by increasing oxidative stress levels[45, 70, 72, 74, 81,82,84].

1.6.3.2 Parthenolide promotes oxidative stress

Oxidative stress is characterized by a deregulation of redox homeostasis resultant from enhanced production of reactive oxygen species (ROS) and reactive nitrogen species (RNS) and/or impaired function in antioxidant defenses[85,86]. This redox imbalance is present in various cancer cells, being related to oncogenic stimulation. Indeed, DNA mutations resultant from oxidative stress are a critical step in carcinogenesis and elevated levels of oxidative DNA lesions are detected in many malignancies, which supports the role of ROS in cancer etiology. However, although ROS are predominantly implicated in lipid, protein, and genetic damage, they also play an important role in several aspects of intracellular signaling regulating cell survival and death[55,81].

Having this in mind, PRT is a possible option for cancer treatment since it modulates NF-kB activation and redox homeostasis by promoting ROS production [activates Nicotinamide adenine dinucleotide phosphate hydrogen (NADPH) oxidase[81]] and reducing the intracellular pools of antioxidant defenses [covalently interacts with thioredoxin, glutamate-cysteine ligase, glutathione peroxidase, glutathione S-

transferase, and reduced glutathione (GSH)[82,84]][45, 70, 72,74]. One important effect of this mechanism is the dissipation of mitochondrial membrane potential, which will then promote the release of cytochrome c and induce the intrinsic apoptotic pathway[45, 55,74].

Since PRT has the selective[52, 62, 68–70, 73,76] ability to simultaneously target two molecular mechanisms in several tumor cell types, such as leukemias[52,73] (ALL[75], acute myeloblastic leukemia[54,62]), lymphomas[73] (EBV-positive BL[47,48]), multiple myeloma[52, 62,76], cholangiocarcinoma[54], and breast[54,76], lung[54], prostate[54], and pancreatic cancers[76], it represents an exciting research opportunity for the development of a new therapeutic approach. In addition, the mediated sensitization to other anti-tumor regimens, allowing the use of lower toxicities while the efficacy is maintained, is another appealing characteristic of this compound[47, 54,76].

1.7 Objective

Despite the increased knowledge regarding the etiology of several lymphoid malignancies and the constant design and study of promising treatment options which consider important genetic and molecular changes, the response rates to conventional chemotherapy are still unsatisfactory and are frequently associated with chemoresistance, considerable (long-term) toxicity, and/or relapse. Therefore, new therapeutic alternatives are still a need. PRT will be a possible option since it has a double anti-tumor effect, in a selective way, interfering with NF-kB, a very important signaling pathway, and inducing an oxidative stress state that promotes the death of malignant cells. Finally, PRT can also be a good strategy to enhance the anti-tumoral activity of several conventional therapies since a synergistic effect has already been described in solid tumors such as lung and gastric cancer.

As such, the aim of this study was to evaluate the therapeutic potential of PRT on acute lymphoblastic leukemia and Burkitt lymphoma cell lines, and to characterize the type of cell death induced as well as its molecular mechanisms.

Materials & Methods

2. Materials & Methods

2.1. Characterization and culture of malignant hematological cell lines

For this study, six cell lines were used: 697 and KOPN-8 as an *in vitro* model of B-ALL; CEM, JURKAT and MOLT-4 as a model of T-ALL; and RAJI as a model of BL.

The 697 cell line [German Collection of Microorganisms and Cell Cultures (DSMZ)] was established from the bone marrow of a 12-year old boy with pre-B-ALL at first relapse. This is a pseudodiploid cell line with expression of the fusion gene *TCF3-PBX* (*E2A-PBX*) resultant from a translocation between chromosome 7 and 19 [t(1;19)(q23;p13)][87,88]. Beside this, 697 cells express *BCL2*, *BCL3* and c-*MYC* mRNA.

The KOPN-8 cell line (DSMZ) was established from the peripheral blood of a 3-year-old girl with pre-B-ALL, expressing, like 697 cell line, cytoplasmic IgM and early B lineage-restricted antigens (CD10 and CD19). This is an human hypodiploid cell line which carries a translocation between chromosome 11 and 19 [t(11;19)(q23;p13)] leading to the *MLL-MLLT1* fusion gene[88].

The CCRF-CEM cell line, also known as CEM [American Type Culture Collection (ATCC)], was established from the peripheral blood of a 4-year-old female with mature T-ALL at diagnosis. This lymphoblastic cells are near-diploid and express T cells' surface antigens (CD3, CD4, CD5, CD7 and $TCR_{\alpha/\beta}$)[89].

The JURKAT cell line (ATCC), originally designed JM, was established from the peripheral blood of a 14-year-old boy with mature T-ALL at first relapse[90]. Regarding cytogenetics these cells have a hypotetraploid karyotype.

The MOLT-4 cell line (ATCC) was established from the peripheral blood of a 19-year-old man with thymic T-ALL[91,92] in relapse after multidrug chemotherapy[93]. This human cell line is hypertetraploid[92] and possess a missense mutation (G→A, Arg→His) at codon 248 of the *TP53* gene[91]. MOLT-4 has immunophenotypic characteristics of thymocytes with strong expression of CD1 and CD5 as well as variable expression of CD4 and CD8[92].

The RAJI cell line (ATCC) was established from a BL of the left maxilla of an 11-year-old African male[94–96]. This lymphoblast-like cell line[94,95] is hypotetraploid and is

described to carry a translocation between chromosome 8 and 14 [t(8;14)] leading to *MYC-IGH* fusion gene. Immunophenotypically, RAJI cells express B cell markers (CD19, CD20 and CD79a) and some proteins related with their antigen presenting activity [human leukocyte antigen-D related (HLA-DR) and CD80]. Besides this, CD10, a surface protein used to confirm the BL diagnosis, is also expressed.

All cell lines were maintained in suspension culture in Roswell Park Memorial Institute 1640 (RPMI 1640) medium (Lonza), containing 2 mM L-glutamine, 20 mM 4-(2-hydroexyethyl)-1-piperazineethanesulfonic acid (HEPES), 1.5 g/L sodium bicarbonate ($NaHCO_3$), 100 U/mL penicillin, 100 µg/mL streptomycin, and supplemented with 10% heat-inactived fetal bovine serum (FBS) (Gibco). Cells were grown at their optimal growth density and maintained at 37°C in a humidified atmosphere containing 5% carbon dioxide (CO_2).

2.2. Incubation of the cell lines with Parthenolide

The different cell lines were platted at their optimal growth density (697 and JURKAT at 0.5 million cells/mL, KOPN-8 at 0.3 million cells/mL, CEM and RAJI at 0.25 million cells/mL, and MOLT-4 at 0.2 million cells/mL) and then incubated in absence or presence of different concentrations of PRT [stock solutions were prepared with dimethyl sulfoxide (DMSO) and stored at - 20°C] in single dose or daily administration for a period of 72 hours (Table 5).

2.3. Analysis of Parthenolide's effect on cellular metabolic activity by resazurin assay

After incubation of all the cell lines under the conditions stated bellow, cell viability was indirectly determined using the resazurin assay.

Table 5 – Incubation conditions of the cell lines with Parthenolide

Concentrations (μM)	Cell Lines					
	697	CEM	JURKAT	KOPN-8	MOLT-4	RAJI
PRT 1	✓	✓	✓	✓	✓	✓
PRT 0.7*				✓		✓
PRT 2				✓		✓
PRT 2.5	✓			✓		
PRT 1*		✓				
PRT 3		✓				
PRT 1.3*	✓					
PRT 4	✓					
PRT 5	✓	✓	✓	✓	✓	✓
PRT 2*					✓	
PRT 6					✓	
PRT 7.5					✓	
PRT 10	✓	✓	✓	✓	✓	✓
PRT 4*			✓			
PRT 12			✓			
PRT 25	✓	✓	✓	✓	✓	✓
PRT 50	✓	✓	✓	✓	✓	✓
PRT 75	✓	✓	✓	✓	✓	✓
PRT 100	✓	✓	✓	✓	✓	✓

To evaluate the therapeutic potential of Parthenolide on malignant hematological cell lines, cells were incubated in absence or presence of different concentrations of PRT in single dose and daily administration for a period of 72 hours. In the single administration scheme, the PRT concentrations used were the same for all cell lines and consisted of 1, 5, 10, 25, 50, 75, and 100 μM. In the case of the daily administration, the half maximal inhibitory concentration (IC_{50}) at 72 hours was divided into three administrations every 24 hours (*), which were compared with the single administration of the IC_{50} at the same timepoint.

Regarding the cell death, cell cycle, oxidative stress and NF-kB levels analysis, cells were incubated, for 24 hours, in absence or presence of the concentrations in red (✓).

Resazurin (Sigma-Aldrich), also known as Alamar Blue, is a cell permeable redox indicator that fluoresces and changes color upon reduction by viable metabolic active cells[97–101]. Therefore, the intracellular conversion of resazurin (non-fluorescent blue form) into resorufin (highly fluorescent pink form)[98–101] by mitochondrial [NADPH, nicotinamide adenine dinucleotide hydrogen (NADH), flavin adenine dinucleotide hydrogen (FADH), flavin mononucleotide hydrogen (FMNH), and numerous

cytochromes][99,100] and cytosolic[99] reductases can be measured and may provide an idea of the number of viable cells present, since the rate of dye reduction is directly proportional to the metabolic competence of cell cultures[98,100].

Thus, a volume of resazurin at 0.2 mg/mL was added to the cultured cells at each 24-hour period. After 2 to 5 hours of incubation with the dye, depending on the cell line in question, the intensity of reduced resazurin was measured at 600 and 570 nm on a microplate spectrophotometer (Synergy™ HT Multi-Mode Microplate Reader, Biotek Instruments). The metabolic activity on each condition was calculated according to the equation 1

$$Metabolic\ Activity\ (\%) = \frac{A_{[570-600]}\ sample - A_{[570-600]}\ blank}{A_{[570-600]}\ control - A_{[570-600]}\ blank}\ x\ 100 \quad \text{, equation 1}$$

where A_{570} corresponds to the absorbance at λ = 570 nm and A_{600} to the absorbance at λ = 600 nm. The results of each test represent the average of 3 readings and 5 independent experiments were performed.

2.4. Cell death analysis

To access cell death induced by PRT, we used optical microscopy, through the study of morphological characteristics, and flow cytometry (FC), using annexin-V/7-AAD double staining and the JC-1 probe. Besides this, FC was also used to evaluate some apoptotic proteins' expression levels [FAS cell surface death receptor (FAS), FAS ligand (FAS-L), and activated caspase-3], clarifying the molecular mechanisms involved.

2.4.1 Cell death analysis by flow cytometry using annexin-V/7-AAD double staining

Annexin-V/7-AAD double staining is a widely-used protocol to study apoptotic and/or necrotic cells through differences in phospholipid distribution and plasma membrane

integrity and permeability[102–105]. Annexin-V is a calcium-dependent phospholipid-binding protein with high affinity for phosphatidylserine (PS), which is translocated from the inner side of the plasma membrane to the surface in one of the earlier events of apoptosis[103–105]. 7-amino actinomycin D (7-AAD)[102,105] is a vital dye that allows the identification of early and late apoptotic cells. Its ability to enter a cell is dependent of the integrity of the plasma membrane, which is decreased in later stages of cell death (apoptosis or necrosis)[103–105]. Therefore, viable cells with intact membranes are both annexin-V and 7-AAD negative, whereas early apoptotic cells are annexin-V positive and 7-AAD negative, and late apoptotic or necrotic cells are both annexin-V and 7-AAD positive. Necrotic cells are 7-AAD positive and annexin-V negative[103,105].

Cell death was assessed after an incubation period of 24 hours under the conditions indicated in Table 5. For that, half a million cells were collected, washed with phosphate-buffered saline (PBS) and centrifuged for 5 minutes at 1 736 x G. Then, cells were incubated in 100 µL of annexin-V binding buffer [0.1 M HEPES, 1.4 M sodium chloride (NaCl) and 25 mM calcium chloride ($CaCl_2$)] with 2.5 µL annexin-V-APC (BioLegend) and 5 µL 7-AAD (BD Bioscience) for 15 minutes in the dark. After this, 300 µL of the same buffer were added and 25 000 events were acquired in FACS Calibur (Becton Dickinson). Results were analyzed in Paint-a-Gate™ software (BD Biosciences) and are expressed as percentage of live cells, early apoptotic cells, necrotic cells, and late apoptotic/necrotic cells, representing the mean ± standard error of 3 independent experiments.

2.4.2 Cell death analysis by optical microscopy

After smearing the different cell lines and staining the slides according to May Grünwald-Giemsa protocol, the analysis of cell morphology was performed by optical microscopy.

For this, after an incubation period of 24 hours under the conditions indicated in Table 5, half a million cells were collected and centrifuged for 5 minutes at 15 115 x G. Then, cells were washed with PBS by centrifugation and resuspended in a small amount of FBS in order to facilitate adhesion to the slides. Smears were performed and, after

drying, were stained with May Grünwald reagent (Sigma-Aldrich) during 3 minutes followed of washing with 1.5 mL of mili-Q water for 1 minute. Then, slides were stained with Giemsa solution (Sigma-Aldrich) (1:8 dilution with mili-Q water) for 15 minutes. Slides were washed with water and dried in vertical position until observation.

Finally, cells were visualized at 1 000 x magnification in Nikon Eclipse 80i microscope coupled with Nikon Digital Camera DXm 1200F, where pictures were acquired using the NIS-Elements Microscope Imaging Software v4.3.

2.4.3 Mitochondrial membrane potential analysis by flow cytometry

Besides plasma membrane composition and integrity alteration, disruption of active mitochondria is other characteristic of apoptosis. Taking the changes in mitochondrial membrane potential into account, the membrane-permeant 5,5',6,6'-tetrachloro-1,1',3,3'-tetraethylbenzimidazolcarbocyanine iodide[106,107] (JC-1) dye can be used to monitor mitochondrial dysfunction since it accumulates in this organelle in a potential-dependent manner. In the presence of cell death, due to the loss of membrane polarization, JC-1 is not internalized and is predominantly in the monomer (M) form that emits green fluorescence (527 nm). Conversely, in the presence of viable cells JC-1 is mainly internalized and presents in the aggregate (A) form emitting a red to orange color (590 nm)[106,108].

Thus, after incubation as stated above (Table 5), half a million cells were washed with PBS and incubated with 1 µL JC-1 (Sigma-Aldrich; 5 mg/mL) for 15 minutes at 37˚C. Afterwards, cells were washed with PBS and centrifuged for 5 minutes at 1 736 x G. Then, 300 µL of PBS were added and 25 000 events were acquired in FACS Calibur (Becton Dickinson). Results were analyzed using Paint-a-Gate™ software (BD Biosciences) and are expressed as the ratio between the mean fluorescence intensity (MFI) of monomers and aggregates, representing the mean ± standard error of 3 independent experiments.

2.4.4 Apoptotic proteins' expression levels analysis by flow cytometry

In order to assess the molecular mechanisms behind PRT's cytotoxicity, FC using monoclonal antibodies associated with fluorochromes can be very useful. Indeed, it makes possible the evaluation of the levels of some molecules involved in cell death processes such as FAS and its ligand (FAS-L), which are involved in the formation of a death-inducing signaling complex, and caspase-3, a pro-apoptotic enzyme which plays a central role in the execution-phase of apoptosis.

2.4.4.1 Activated caspase-3

After incubation as stated in Table 5, half a million cells were washed with PBS and incubated with 50 µL of fixation solution (Solution A, Intracell Kit, Immunostep) for 15 minutes in the dark. After washing again, cells were incubated with 50 µL of permeabilization solution (Solution B, Intracell Kit, Immunostep) and 10 µL of PE-labelled anti-activated caspase-3 monoclonal antibody (BD Biosciences), for 15 minutes in the dark. Finally, cells were washed with PBS and resuspended in 300 µL of the same buffer solution.

25 000 events were acquired in FACS Calibur (Becton Dickinson) and results were analyzed using Paint-a-Gate™ software (BD Biosciences). Results are expressed as the percentage of positive cells for the activated caspase and as its levels (MFI), representing the mean ± standard error of 3 independent experiments.

2.4.4.2 FAS and FAS ligand

Half a million cells incubated for 24 hours in absence or presence of PRT (Table 5) were washed with PBS and incubated with 10 µL FAS-FITC (BD Biosciences) and 10 µL FAS-L-PE (Santa Cruz Biotechnology) for 15 minutes in the dark. Then, cells were washed and resuspended in 300 µL PBS. 25 000 events were acquired in FACS Calibur (Becton Dickinson) and results were analyzed in the Paint-a-Gate™ software (BD Biosciences).

Results are expressed as MFI of FAS and FAS-L variation and represent the mean ± standard error of 3 independent experiments.

2.5 Oxidative stress analysis by flow cytometry

The effect of PRT-induced cell death through oxidative stress was evaluated using a series of probes that allow the detection of reactive oxygen species (superoxide anion and peroxides) and antioxidants' (reduced glutathione) levels.

Dihydroethidium (DHE) is a blue dye used to monitor superoxide anion production since it can diffuse across cell membranes and upon reaction with superoxide is dehydrogenated to ethidium, a red fluorescent product which intercalates into DNA, staining the nucleus bright fluorescent red[109,110].

2',7'-dichlorodihydrofluorescein diacetate ($DCFH_2DA$) is an esterified compound which can freely cross cell membrane. In cytosol, it is hydrolyzed by intracellular esterases in 2',7'-dichlorodihydrofluorescein ($DCFH_2$) becoming trapped inside the cell. Then, in the presence of reactive oxygen species, particularly hydrogen peroxide (H_2O_2), it is oxidized in 2',7'-dichlorofluorescein (DCF), which emits green fluorescence upon excitation[106,110–112].

1-(4-chloromercuriophenylazo)-2-naphthol (mercury orange) is a mercurial compound which binds to the GSH through its sulfhydryl groups, forming fluorescent orange adducts[112].

Cells were incubated, for 24 hours, in the absence and presence of PRT (Table 5). Half a million cells were washed with PBS and 2.5 µL DHE (Sigma-Aldrich; 10 mM), 1 µL $DCFH_2DA$ (Molecular Probes, Invitrogen; 50 mM), and 5 µL mercury orange (Sigma-Aldrich) were administered. After incubation for 15 minutes (DHE and mercury orange) or 45 minutes ($DCFH_2DA$) at 37˚C, cells were washed with PBS and centrifuged for 5 minutes at 1 736 x G. Then, 300 µL of PBS were added and 25 000 events were acquired in FACS Calibur (Becton Dickinson). Results were analyzed using Paint-a-Gate™ software (BD Biosciences) and are expressed as MFI of superoxide, hydrogen peroxide, and

reduced glutathione normalized to the control, representing the mean ± standard error of at least 2 independent experiments.

2.6 Cell cycle analysis by flow cytometry

The antiproliferative effect of PRT was evaluated by cell cycle analysis, since the quantification of DNA content reveals cells' distribution through the different phases of the cell cycle. This can be achieved using a DNA intercalating dye, like propidium iodide (PI), which binds to double-stranded polynucleotides in proportion to the amount present in the cell[113–115]. As such, cells at the S phase, which have more DNA than cells in G_0/G_1, will take up proportionally more dye and will fluoresce more brightly until they have doubled their DNA content. Cells in G_2/M phase will be approximately twice as bright as cells in G_0/G_1[115,116]. Besides this, with this method is also possible to detect apoptotic cells with fractional DNA content (sub-G_1 peak)[115].

After a 24 hours incubation period under the conditions expressed in Table 5, a million cells were collected, washed with PBS and centrifuged for 5 minutes at 1 736 x G. Cells were incubated in 200 µL of cold 70% ethanol for 30 minutes at 4˚C. Then, cells were washed with PBS and 300 µL of PI/ribonuclease (RNase) solution (Immunostep) were added. 50 000 events were acquired in FACS Calibur (Becton), using CellQuest™, and the analysis of the results was performed in Modfit™ (ModFit LT). Results are expressed as percentage of cells in each phase of the cell cycle (sub-G_1, G_0/G_1, S, and G_2/M), representing the mean ± standard error of 3 independent experiments.

2.7 Analysis of phosphorylated NF-kB levels by flow cytometry

To assess the efficacy of PRT in IKK inhibition, the levels of phosphorylated NF-kB were analyzed using a monoclonal antibody coupled to a fluorochrome. Therefore, cells were incubated in the conditions stated in Table 5 and half a million cells were collected. Cells were washed with PBS and incubated with 50 µL of fixation solution (Solution A,

Intracell Kit, Immunostep) for 15 minutes in the dark. After washing again, cells were incubated with 50 µL of permeabilization solution (Solution B, Intracell Kit, Immunostep) and 2 µL of PE-labelled anti-phosphorylated NF-kB monoclonal antibody (BD Biosciences), for 15 minutes in the dark. Finally, cells were washed with PBS and resuspended in 300 µL of the same buffer solution. 25 000 events were acquired in FACS Calibur (Becton Dickinson) and results were analyzed using Paint-a-Gate^{TM} software (BD Biosciences). Results are expressed as MFI of phosphorylated NF-kB, representing the mean ± standard error of 3 independent tests.

2.8 Statistical analysis

Regarding metabolic activity, the IC_{50} was determined from log dose-response curves using non-linear regression analysis. Analysis of variance (Kruskal-Wallis or two-way ANOVA) was performed to compare experimental data with controls. Dunn's and Dunnet's test correction were used to analyze the effect of time and dose on metabolic activity, respectively. Mann-Whitney test was performed to analyze the effect of the administration scheme, comparing daily and single-dose administration.

Regarding flow cytometry, analysis of variance (Kruskal-Wallis) with Dunn's post-hoc test was performed to compare experimental data with controls in each cell line.

Statistical analysis was performed using GraphPad Prism 6.0 and all data was expressed as mean ± standard error of the number of independent experiments (indicated in the figure legends). A $p<0.05$ was considered statistically significant.

Results

3. Results

3.1. Parthenolide's effect on metabolic activity

The therapeutic potential of PRT on malignant hematological cell lines was determined by the resazurin metabolic assay, in which 697, KOPN-8, CEM, JURKAT, MOLT-4, and RAJI cells were incubated in absence [control (CTL)] or presence of increasing concentrations of PRT (between 1 µM and 100 µM) for a period of 72 hours.

Figure 8 illustrates dose-response curves that represent the relation between number of metabolic active cells (as a percentage of control) and time of exposure to the inhibitor. Thus, for each cell line under study, PRT induced a metabolic activity reduction which was dependent on the concentration, time of exposure (statistically significant for doses superior to 25 µM), and cell line. Indeed, this could be verified by comparing the IC_{50} determined using non-linear logistic regression models. RAJI cells seemed to be the most sensitive to PRT exhibiting a 50% reduction in its metabolic activity after a 24 hour incubation period with 34.5 µM of PRT (Figure 8). This also happened with CEM, KOPN-8, 697, and MOLT-4 cell lines. However, these cell lines required a higher dose of PRT to reach the IC_{50}, which was 45.6 µM for CEM, 72.3 µM for KOPN-8, 89.0 µM for 697, and 94.3 µM for MOLT-4. For JURKAT cells the IC_{50} (30.2 µM) was only reached at 48 hours of incubation. After 72 hours of incubation, cell lines' sensitivity was somewhat different, being KOPN-8 cells the most sensitive (IC_{50} = 2.0 µM). At this timepoint, RAJI, CEM, 697, MOLT-4, and JURKAT cell lines reached the IC_{50} with 2.2, 3.0, 3.5, 6.0, and 12.4 µM PRT, respectively (Figure 8).

Subsequently, it was assessed whether the scheme of administration influenced PRT's effect on metabolic activity. For that, lower concentrations of PRT (equivalent to one third of the IC_{50} at 72 hours) were administered every 24 hours, establishing a comparison between this daily administration and the single administration of the determined IC_{50} concentration at the same timepoint. When comparing with single administration, daily administration did not induce a significant reduction in cellular metabolic activity (Figure 9).

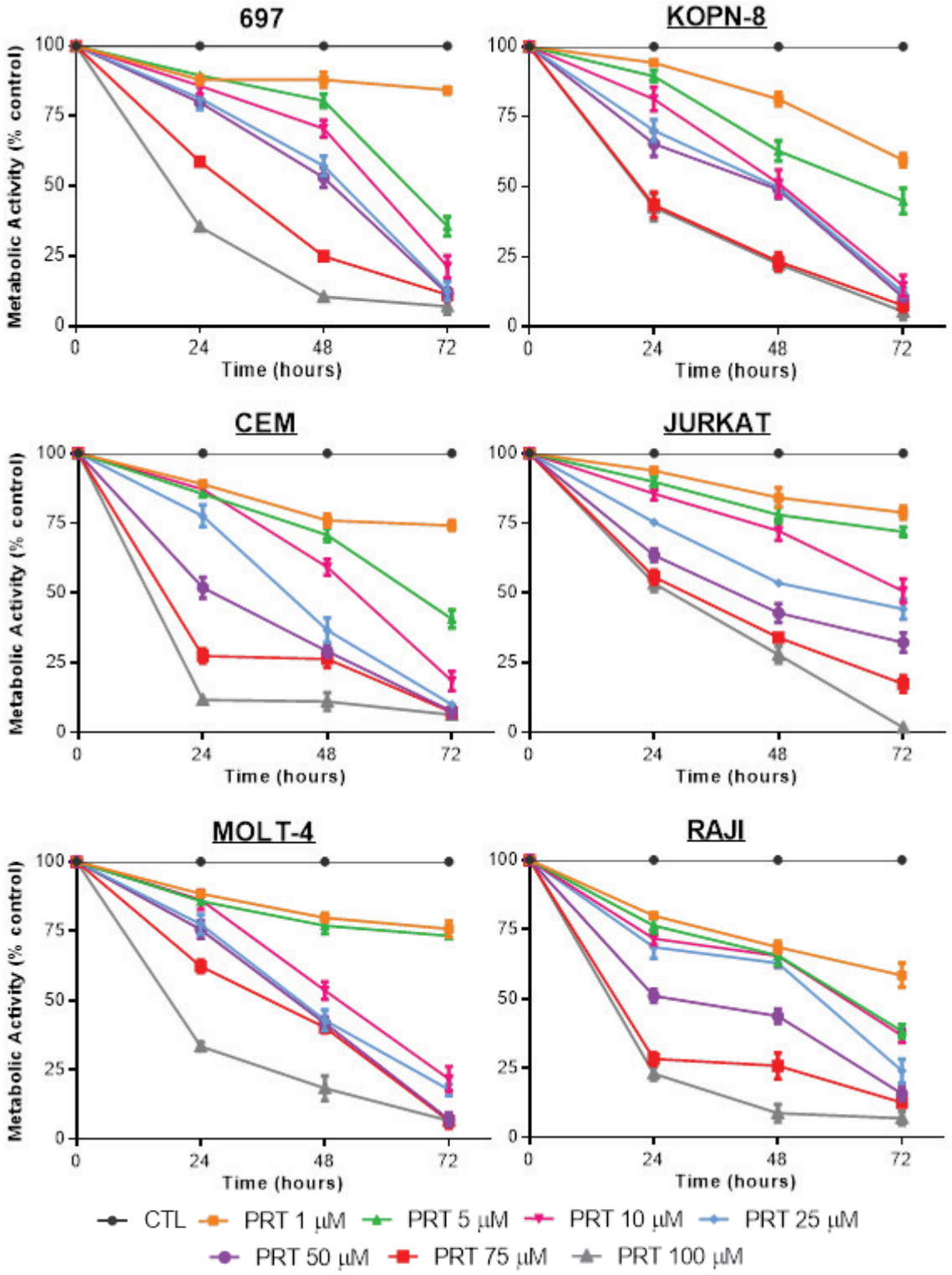

Figure 8 – Parthenolide's effect on the metabolic activity of ALL and BL cell lines. The different cell lines were incubated at their optimal growth density, in the absence and presence of increasing concentrations of Parthenolide, for a period of 72 hours. Dose-response curves were established by the resazurin metabolic assay each 24 hours, as described in the Materials and Methods section. The results are expressed as a percentage (%) normalized to CTL, representing the mean ± standard error of 5 independent assays.

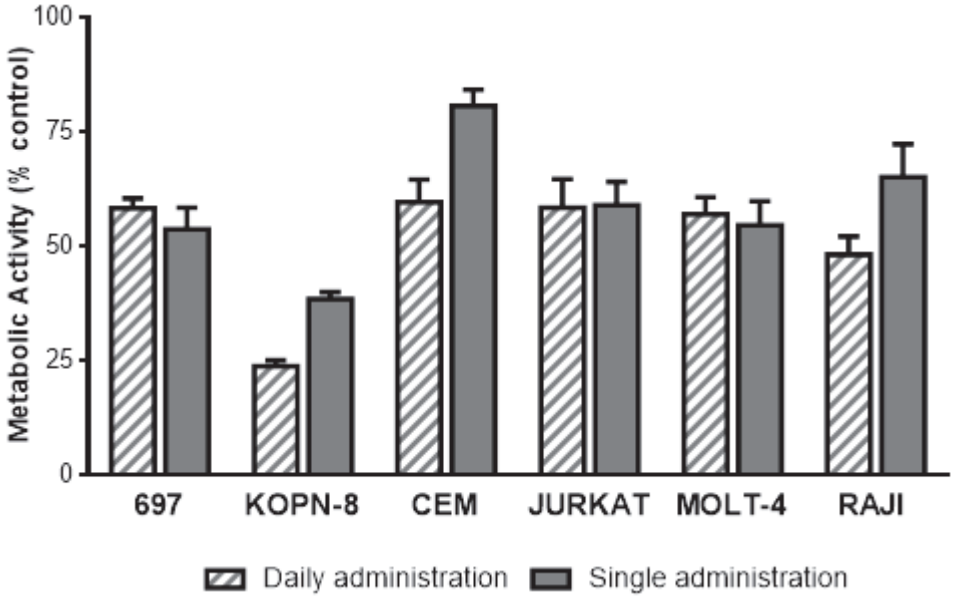

Figure 9 – Parthenolide's daily administration effect on metabolic activity after 72 hours incubation of ALL and BL cell lines. The different cell lines were incubated at their optimal growth density and Parthenolide was administered in single or daily dose administration. Dose-response curves were established by the resazurin assay each 24 hours, as described in the Materials and Methods section. The results are expressed as a percentage (%) normalized to control, representing the mean ± standard error of 5 independent assays.

3.2. Cell death analysis by flow cytometry using annexin-V/7-AAD double staining

A very important feature of anticancer therapies is the cell death promotion, attempting to eradicate malignant cells. Therefore, PRT's cytotoxic effect was accessed by FC, using annexin-V/7-AAD double staining. Since the administration of PRT's concentrations corresponding to the determined IC_{50} at 48 hours induced a lot of cell death by apoptosis, we opted to analyze the cytotoxic effect after a 24 hours incubation in absence or presence of one concentration that induced a little reduction in cellular viability (1 µM) and one that caused a reduction of about 50% in the number of live cells in order to study the molecules associated with PRT-induced cell death.

Thus, as it can be seen in Figure 10, PRT decreased the number of live cells with a parallel increase in cell death predominantly by apoptosis, when comparing with the respective control. Variations in the number of apoptotic cells, mainly the ones in early

apoptosis were observed in all cell lines, being this effect dependent on dose and cell line. KOPN-8 cells seemed to be the most sensitive cell line exhibiting a more pronounced reduction in its viability (an approximately 40% reduction in the number of live cells) comparing the results obtained for PRT 1 µM condition (Figures 10-B and 10-C). As such, increasing PRT dose to 2.5 µM led to a much more pronounced cytotoxic effect, existing not only an increase in apoptotic cells but also in the number of necrotic cells (Figure 10-C). RAJI cells appear to be the less sensitive cell line to PRT's cytotoxic effect. In fact, RAJI cells were rather resistant to 1 µM PRT (Figures 10-B and 10-C). Besides this, the concentration needed to achieve a 50% viability reduction was much higher (10 µM) than those used for the remaining lines (1.3, 2, and 4 times higher than in the case of MOLT-4, CEM and JURKAT, and 697, respectively). The discrepancies between resazurin assay and FC results regarding cellular sensitivity to PRT, are, possibly, due to the fact that cells in initial apoptotic stages still have functional mitochondrial (and cytosolic) reductases which are able to convert resazurin into resofurin, making it impossible to discriminate them from viable cells.

3.3. Cell death analysis by optical microscopy

To confirm the results obtained regarding the type of cell death induced by PRT, cell morphology was analyzed by optical microscopy, using the May-Grünwald Giemsa staining.

In agreement with FC studies, optical microscopy studies revealed that 24 hour incubation with PRT induced morphological changes typical of apoptosis. Thus, by establishing a comparison with the control, it was possible to verify the presence of several protrusions of the cell membrane (blebs) (Figure 11) that will carry larger fragments of nucleus and of various cellular organelles, giving rise to apoptotic bodies. Nuclear fragmentation and apoptotic bodies were also detected (Figure 11). In some PRT conditions, malignant cells also presented cytoplasmic vacuolization, which might be related to drug-induced toxicity or to the onset of the autophagic process. In some

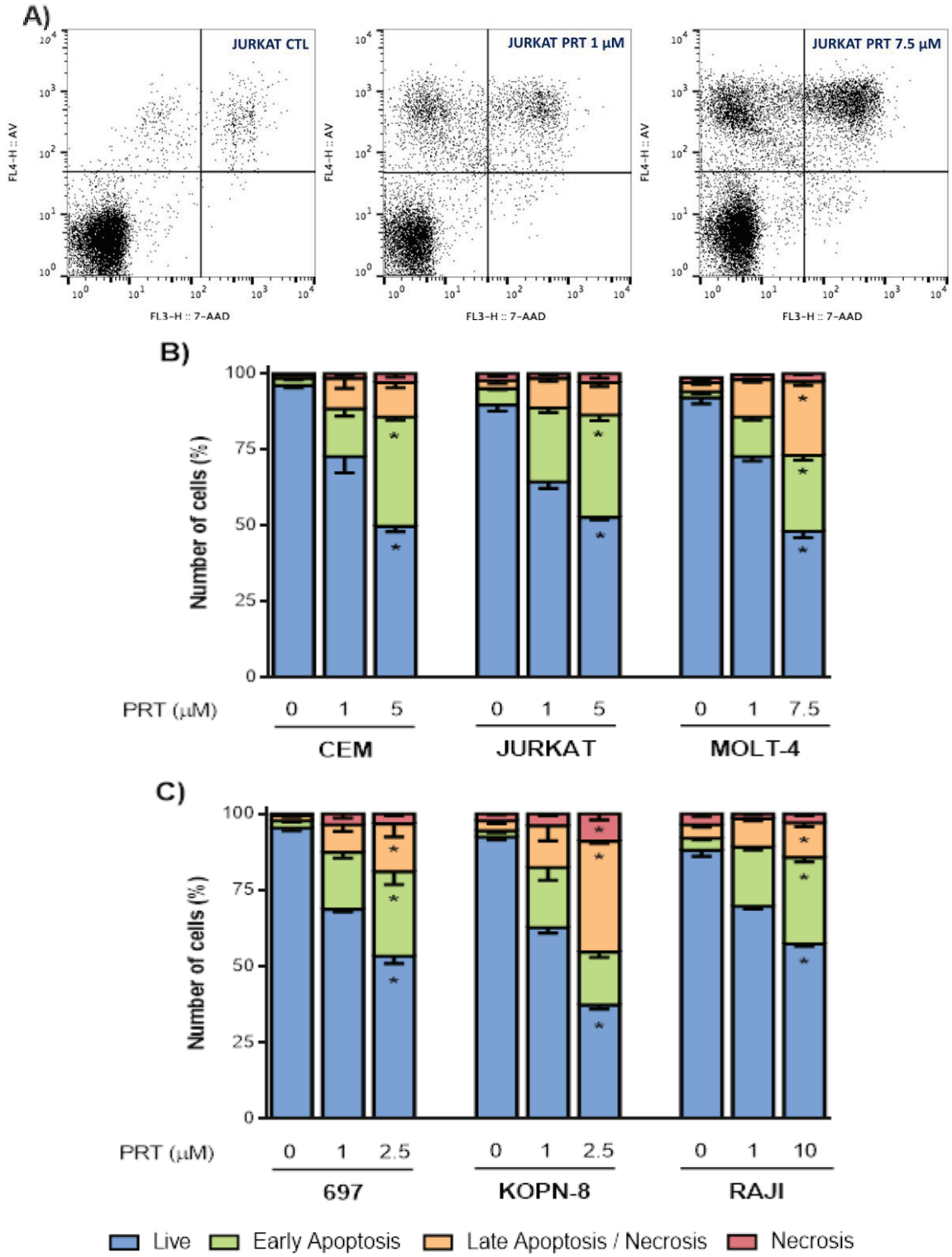

Figure 10 – Parthenolide's cytotoxic effect evaluation in malignant hematological cell lines. The different cell lines were incubated for 24 hours in the absence or presence of different concentrations of Parthenolide as noted in the Figure. Subsequently, cell death was detected by annexin-V/7-AAD double staining as described in the Materials and Methods section. **(A)** Representative example of the dot plots obtained. **(B) (C)** The results are expressed as percentage and represent the mean ± standard error of 3 independent experiments. Statistical analysis was carried out by Kruskal-Wallis with Dunn's post-hoc test. *, $p<0.05$

cases, especially in MOLT-4 treated with PRT 7.5 µM, it was possible to observe catastrophic mitosis, representing cell cycle arrest.

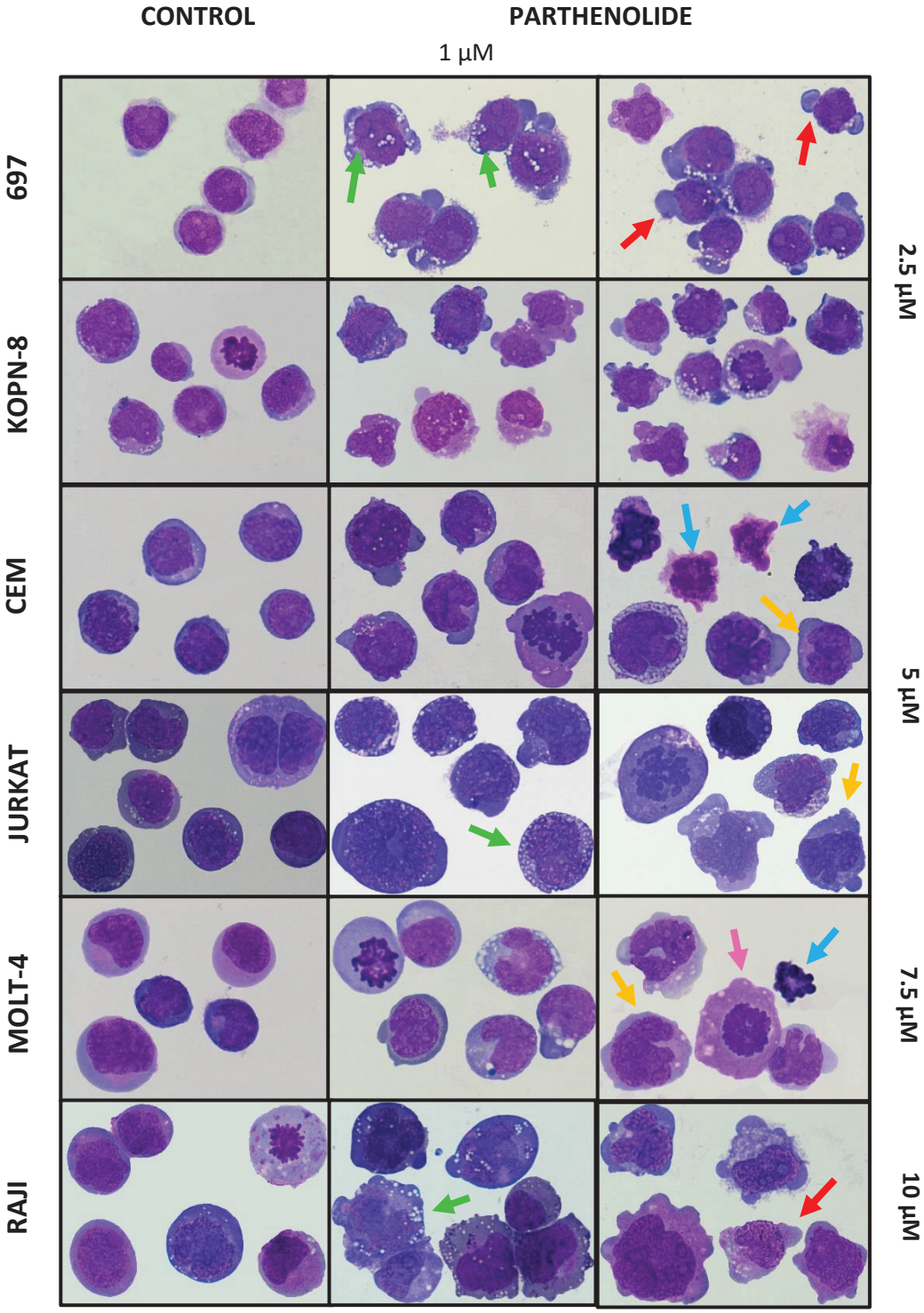

Figure 11 – Cell morphology analysis by optical microscopy in ALL and BL cell lines. Cells were incubated for 24 hours in absence or presence of different concentrations of Parthenolide as depicted in the Figure. May-Grünwald-Giemsa staining was performed as described in the Materials and Methods section. The cells were analyzed by light microscopy (1 000x magnification). Blebbing; nuclear fragmentation; apoptotic bodies; cytoplasmic vacuolization; catastrophic mitosis.

3.4. Caspase levels analysis by flow cytometry

To further confirm the cell death mechanisms induced by PRT, levels of activated caspase-3, a programmed cell death effector protein, were also evaluated by FC.

Results shown in Figure 12 revealed that PRT treatment induced a significant increase in activated caspase-3 levels (Figure 12-A), as well as in the percentage of cells with activated caspase-3 (Figure 12-B). The observed increase was dose dependent and statistically significant, when compared to untreated conditions in the six tested cell lines. Indeed, a higher dose administration induced an increase of 3.16- (p=0.017), 3.87-fold (p=0.015), 6.25- (p=0.017), 9.48- (p=0.015), 12.88- (p=0.003), and 22.18- (p=0.014) in JURKAT, RAJI, KOPN-8, CEM, MOLT-4, and 697's percentage of positive cells for activated caspase-3, respectively. Similarly, same doses increased the levels of this caspase in all cell lines [1.26-fold in RAJI, 1.71-fold (p=0.014) in JURKAT, 1.88-fold (p=0.007) in MOLT-4, 2.04-fold (p=0.027) in CEM, 2.29-fold (p=0.023) in KOPN-8, and 2.35-fold in 697 cells]. Another thing to note is that the basal intracellular levels of caspase-3 were cell line-dependent, presenting JURKAT cells higher levels of this pro-apoptotic protein.

3.5. FAS and FAS-L expression levels evaluation by flow cytometry

To infer the involvement of the extrinsic apoptotic pathway in PRT-induced cytotoxicity, the levels of FAS receptor and its ligand (FAS-L) were analyzed by FC.

As noted in Figure 13, the apoptotic pathway initiated by FAS and FAS-L interaction was not equally involved in cell death inducted by PRT, since there was no significant increase in the levels of these proteins in CEM and JURKAT cell lines. Conversely, this pathway seemed to play an active role in the induction of apoptosis in MOLT-4 and RAJI cells, as well as in B-ALL *in vitro* models (697 and KOPN-8), since there was a considerable increase in FAS [2.5 µM incubation induced a 2.17- and 2.62-fold (p=0.032) increase in KOPN-8 and 697 cells, respectively; and 7.5 µM led to an increase of 1.15-fold (p=0.013) in MOLT-4 cells] (Figure 13-A) and FAS-L levels [higher dose incubation induced an

increase in 1.38-fold in RAJI, 1.62-fold in KOPN-8, 2.14-fold (p=0.013) in MOLT-4, and 2.57-fold in 697 cells] (Figure 13-B). Another thing to note is that the levels of the surface death receptor were cell line-dependent, presenting MOLT-4 and RAJI cells higher levels, which suggest a greater propensity for the occurrence of programmed cell death induced by the extrinsic pathway.

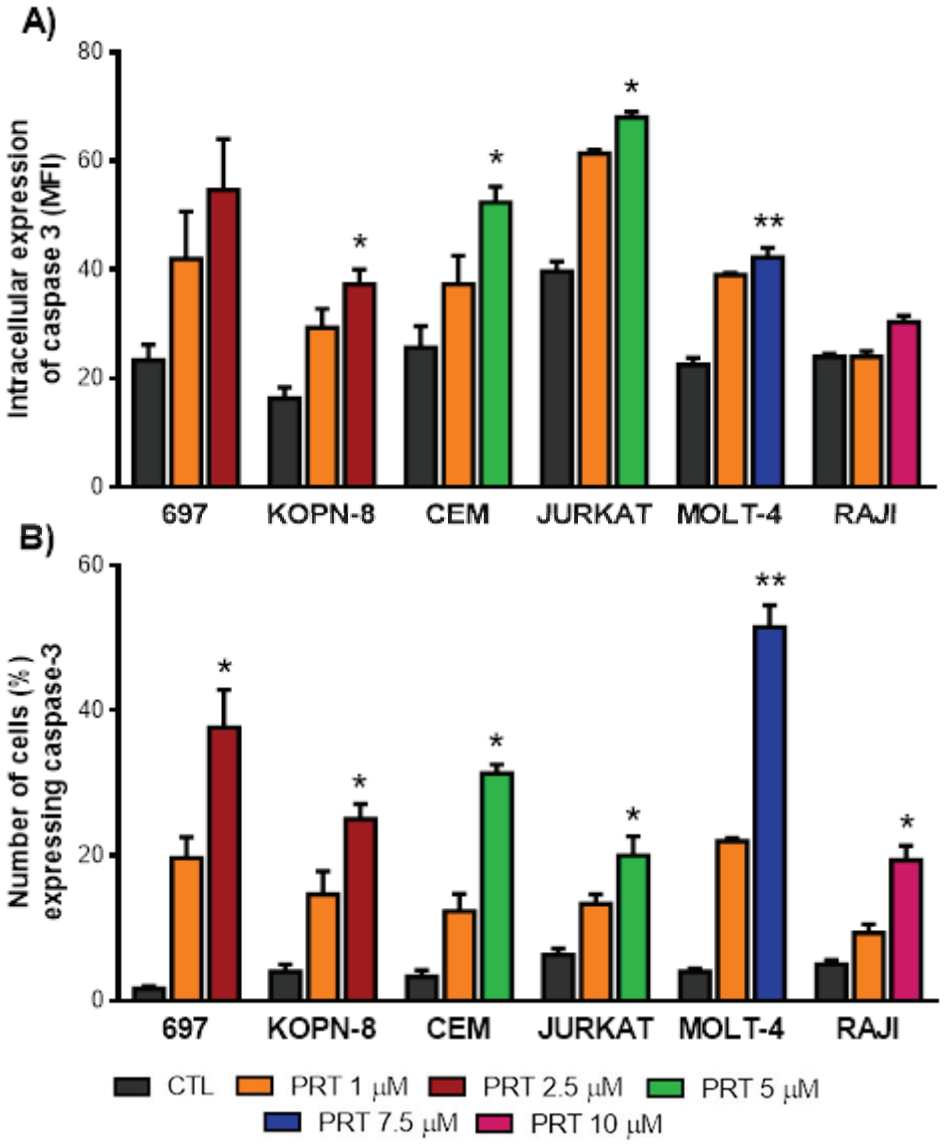

Figure 12 – Activated caspase-3 levels in malignant hematological cell lines incubated in the absence (control) and presence of Parthenolide. Cells were incubated with Parthenolide for 24 hours and the levels of caspase-3 were analyzed using PE-labelled anti-activated caspase-3 antibody as described in the Materials and Methods section. The results are expressed as mean fluorescence intensity (MFI) (A) and as a percentage of positive cells for cleaved caspase-3 (B), representing the mean ± standard error of 3 independent experiments. Statistical analysis was carried out by Kruscal-Wallis with Dunn's post-hoc test. *, p<0.05; **, p<0.01

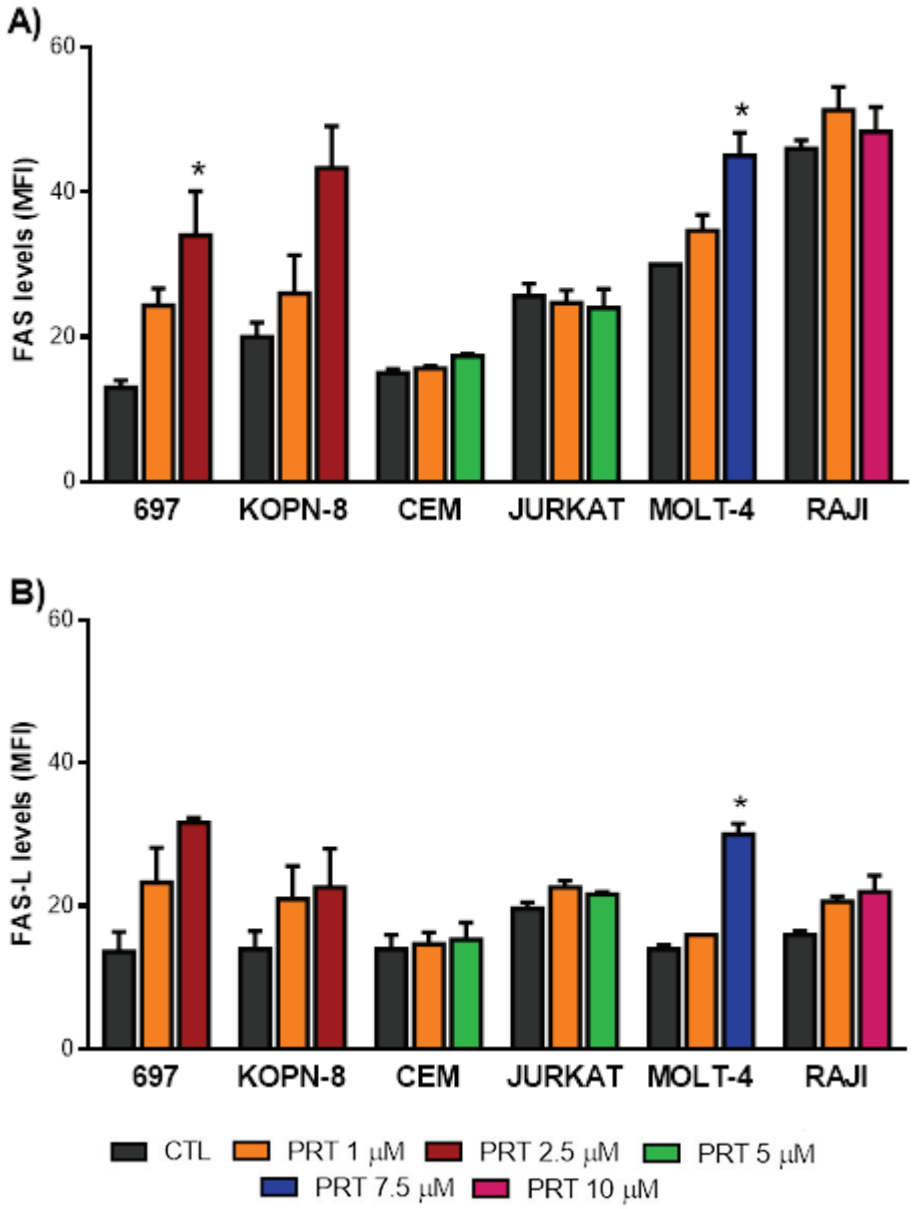

Figure 13 – FAS and FAS-L levels in malignant hematological cell lines incubated in the absence (control) and presence of Parthenolide. Cells were incubated with Parthenolide for 24 hours and the levels of the surface proteins were analyzed using specific antibodies as described in the Materials and Methods section. The results are expressed as mean fluorescence intensity of FAS (A) and FAS-L (B) variation and represent the mean ± standard error of 3 independent experiments. Statistical analysis was carried out by Kruscal-Wallis with Dunn's post-hoc test. *, $p<0.05$

3.6. Mitochondrial membrane potential analysis by flow cytometry

In order to indirectly evaluate a possible involvement of the intrinsic pathway of apoptosis, cells treated with PRT were analyzed by FC after labeling with the JC-1 probe that can coexist in monomeric or aggregate form depending on the mitochondrial membrane potential.

Thus, as illustrated in Figure 14, PRT's administration induced an increase of JC-1 monomers/aggregates ratio under all conditions tested [3.5-fold (p=0.022) in 697 and 3.92-fold (p=0.022) in KOPN-8 cells; 3.79-fold (p=0.022) in CEM, 5.02-fold (p=0.015) in JURKAT, and 6.43-fold (p=0.014) in MOLT-4 cell lines; and 1.33-fold in RAJI cells when incubated with its IC_{50} dose], which translates into a decrease in mitochondrial membrane potential and/or increase in the disruption of active mitochondria, and a consequent activation of the intrinsic pathway of apoptosis. Another thing to note is that the basal M/A ratio was similar in all cell lines, except in RAJI cells where it is approximately 6 times higher.

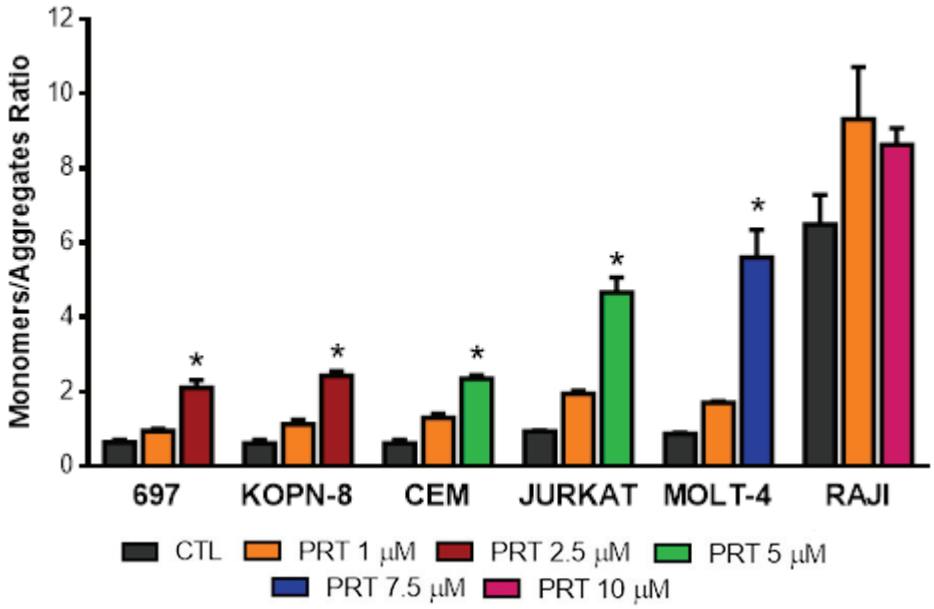

Figure 14 – Mitochondrial membrane potential evaluation in malignant hematological cell lines incubated in the absence (control) and presence of Parthenolide. Cells were incubated with Parthenolide for 24 hours and mitochondrial membrane potential was analyzed using the JC-1 probe as described in the Materials and Methods section. The results are expressed as the ratio between the mean fluorescence intensity of monomers and aggregates and represent the mean ± standard error of 3 independent experiments. Statistical analysis was carried out by Kruscal-Wallis with Dunn's post-hoc test. *, p<0.05

3.7. Cell cycle analysis by flow cytometry

In order to evaluate whether PRT has a cytostatic effect, the distribution of cells through the different phases of cell cycle was analyzed by flow cytometry after labeling with propidium iodide/RNAse solution (Figure 15).

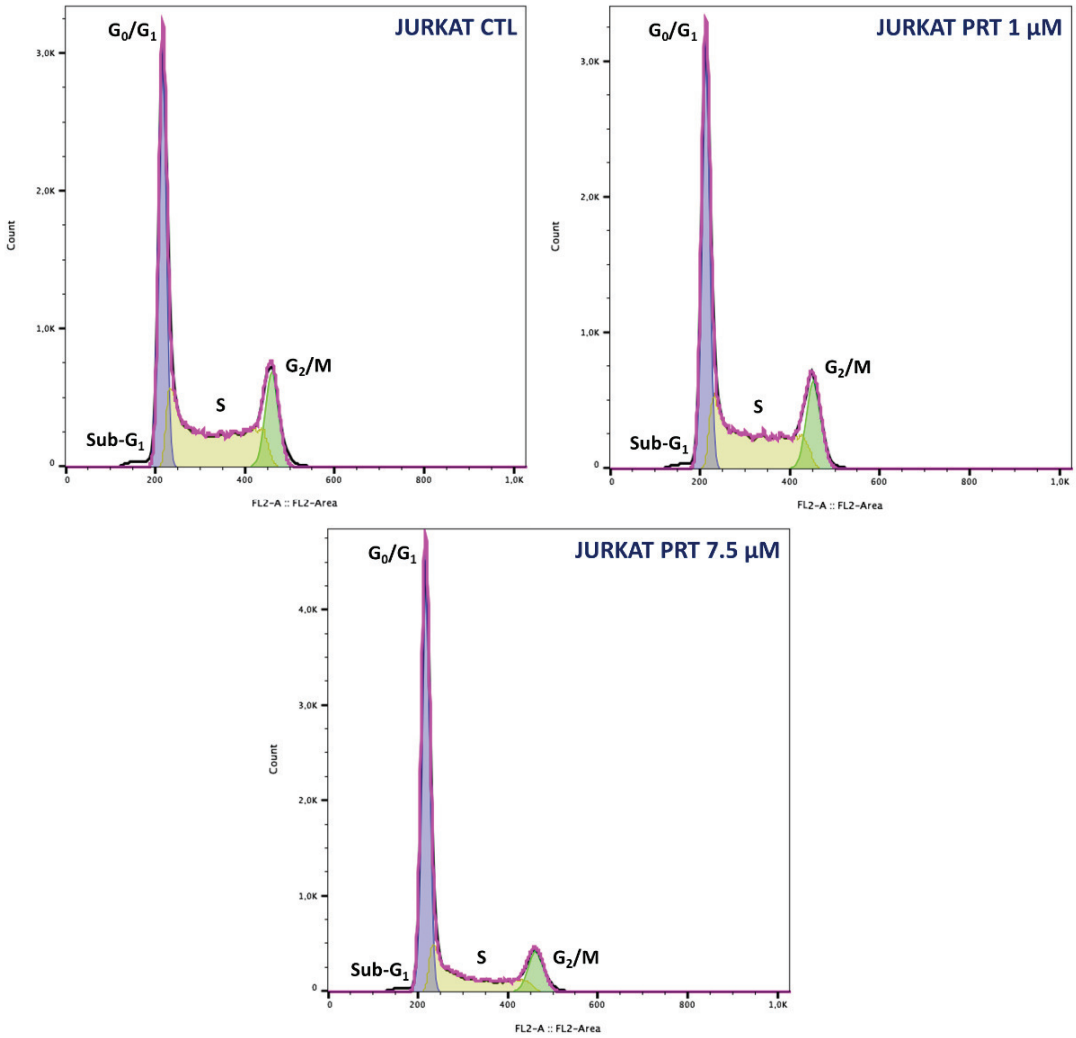

Figure 15 – Representative graphs of cell cycle analysis by flow cytometry after labeling with propidium iodide/RNAse solution

As observed in Table 6, PRT tends to arrest cell cycle progression. When CEM and MOLT-4 cells were incubated with 5 and 7.5 µM of PRT, respectively, there was an anti-proliferative effect translated into an increase in the percentage of cells found in the G_2/M phase, followed by a decrease in G_0/G_1 number of cells (G_2/M cell cycle arrest).

Besides that, the increase in the number of cells in S phase suggested that PRT treated cells had already some difficulty to pass through S phase checkpoint. KOPN-8 and JURKAT cells had a tendency to accumulate in G_0/G_1 phase. On the other hand, PRT's effect in RAJI cell line was concentration dependent. RAJI cells incubated with 1 µM of PRT seemed to arrest at S phase while cells incubated with 10 µM of PRT arrested at G_2/M phase. As to 697 cells PRT seemed to have no effect.

Since cell cycle analysis by flow cytometry using propidium iodide/RNAse allows the detection of apoptotic cells with fractional DNA content, this analysis further confirms that PRT induced cell death by apoptosis. As such, a significant increase in the number of cells undergoing apoptosis (sub-G_1 peak) could be detected when comparing ALL treated conditions to control, where those levels were almost zero. In RAJI cells the sub-G_1 peak was not detected. This may indicate that the cells analyzed are at earlier stages of apoptosis when comparing with the other cell lines (DNA fragmentation is a late event in apoptosis, occurring after PS translocation, blebbing, membrane permeabilization, mitochondria membrane potential disruption, and caspase-3 activation[117–119]) (Table 6).

3.8. Oxidative stress analysis by flow cytometry

In order to infer some of the mechanisms involved in PRT-induced cytotoxicity, intracellular oxidative stress levels were evaluated using a series of probes that allow the detection of reactive oxygen species (superoxide anion and peroxides) and antioxidant defenses (GSH) (Table 7). Moreover, since oxidative stress results from the imbalance between free radicals and antioxidants, ROS/GSH ratio was also determined (Figure 16).

In the presence of increasing doses of PRT, there was an increase of ROS levels comparing with the control. Indeed, the IC_{50} concentrations' administration induced a 1.12-fold increase in 697 (p=0.002) and CEM (p=0.0006), as well as 1.13-, 1.33-, 1.40-, and 1.48-fold increase in superoxide levels in JURKAT (p=0.012), RAJI (p=0.013), MOLT-4 (p=0.001), and KOPN-8 (p=0.003) cells, respectively. Similarly, same dose exposure

Table 6 – Parthenolide's effect on the distribution of cells through the various phases of cell cycle

		Sub-G_1 (% cells)	G_0/G_1 (% cells)	S (% cells)	G_2/M (% cells)
697	CTL	0.0 ± 0.0	68.7 ± 5.5	19.7 ± 6.9	11.7 ± 3.0
	PRT 1 µM	6.7 ± 3.3	72.7 ± 2.3	19.7 ± 6.0	7.7 ± 3.7
	PRT 2.5 µM	12.7 ± 3.5 *	72.3 ± 1.3	19.0 ± 5.5	8.7 ± 4.2
KOPN-8	CTL	1.3 ± 0.9	69.0 ± 4.4	23.0 ± 4.4	8.0 ± 1.0
	PRT 1 µM	6.3 ± 2.0	74.7 ± 2.9	18.3 ± 2.8	7.0 ± 1.5
	PRT 2.5 µM	16.3 ± 1.8 *	77.7 ± 1.2	14.0 ± 1.5	8.3 ± 0.9
CEM	CTL	0.7 ± 0.3	53.7 ± 2.3	35.0 ± 2.9	11.3 ± 2.3
	PRT 1 µM	6.3 ± 1.3	51.3 ± 2.4	35.3 ± 2.9	13.3 ± 1.8
	PRT 5 µM	18.0 ± 4.0 *	43.7 ± 5.5	41.0 ± 4.4	15.3 ± 1.3
JURKAT	CTL	0.3 ± 0.3	43.7 ± 0.3	39.3 ± 1.3	16.0 ± 1.2
	PRT 1 µM	2.0 ± 1.0	47.3 ± 0.7	40.0 ± 1.5	13.7 ± 0.9
	PRT 5 µM	5.7 ± 0.3 *	71.0 ± 1.5 *	21.7 ± 0.3	10.0 ± 0.0 *
MOLT-4	CTL	1.0 ± 2.3	59.3 ± 0.6	35.3 ± 0.9	3.3 ± 1.3
	PRT 1 µM	2.3 ± 1.5	56.3 ± 2.6	37.3 ± 1.3	3.7 ± 0.7
	PRT 7.5 µM	19.0 ± 5.0 *	44.0 ± 4.0 *	42.0 ± 0.6 *	13.7 ± 0.9 *
RAJI	CTL	0.0 ± 0.0	45.7 ± 1.8	42.3 ± 2.0	12.0 ± 1.2
	PRT 1 µM	0.3 ± 0.3	47.7 ± 2.2	46.0 ± 0.6	9.7 ± 0.9
	PRT 10 µM	0.0 ± 0.0	37.7 ± 2.2	41.7 ± 0.3	20.7 ± 1.8

Cells were incubated with PRT for 24 hours and their cell cycle distribution was detected by flow cytometry using PI/RNAse as described in the Materials and Methods section. The results are expressed as percentage of cells in sub-G1 peak as well as G_0/G_1, S, and G2/M phases, and represent the mean ± standard error of 3 independent experiments. Statistical analysis was carried out by Kruskal-Wallis with Dunn's post-hoc test. *, $p<0.05$

increased hydrogen peroxide levels in all cell lines [1.17- (p=0.0007), 1.26- (p=0.0006), 1.37- (p=0.019), 1.43- (p=0.001), and 1.71-fold (p=0.0009) in CEM, KOPN-8, JURKAT, and MOLT-4 cell lines; in RAJI cells the variance was minimal (1.08-fold increase)]. Regarding GSH levels, the IC_{50} doses administration led to 1.34- and 1.41-fold decrease in 697 (p=0.015) and KOPN-8 (p=0.003) cell lines, respectively, as well as a 1.32-, 1.91-, and 2.54-fold and decrease in CEM (p=0.001), MOLT-4 (p=0.002), and JURKAT cells. A 4.21-fold (p=0.005) decrease was also detected in BL *in vitro* model. As observed in Figure 16, the ROS/GSH ratio was increased in all cell lines [2.0- (p=0.015), 2.7- (p=0.022), 3.0-, 3.4-

(p=0.022), 4.5-, and 5.0-fold (p=0.015) in CEM, 697, KOPN-8, JURKAT, RAJI, and MOLT-4, respectively].

Table 7 – Parthenolide's effect in reactive oxygen species and antioxidant defense levels

		SUPEROXIDE ANION (normalized to control)	HYDROGEN PEROXIDE (normalized to control)	REDUCED GLUTATHIONE (normalized to control)
697	CTL	100.0 ± 0.0	100.0 ± 0.0	100.0 ± 0.0
	PRT 1 µM	104.7 ± 1.3	107.2 ± 1.9	84.5 ± 8.5
	PRT 2.5 µM	112.3 ± 3.4 ***	142.7 ± 18.4 **	74.2 ± 5.0 *
KOPN-8	CTL	100.0 ± 0.0	100.0 ± 0.0	100.0 ± 0.0
	PRT 1 µM	123.1 ± 8.0 *	109.4 ± 2.2	92.3 ± 3.3
	PRT 2.5 µM	148.3 ± 17.8 **	125.5 ± 7.4 ***	70.7 ± 6.1 **
CEM	CTL	100.0 ± 0.0	100.0 ± 0.0	100.0 ± 0.0
	PRT 1 µM	103.4 ± 1.3	105.6 ± 2.5	90.4 ± 3.3
	PRT 5 µM	112.4 ± 1.4 ***	117.1 ± 1.4 ***	75.3 ± 4.9 ***
JURKAT	CTL	100.0 ± 0.0	100.0 ± 0.0	100.0 ± 0.0
	PRT 1 µM	109.8 ± 0.4	133.1 ± 2.4	102.3 ± 6.0
	PRT 5 µM	112.7 ± 0.1 *	136.8 ± 1.1 *	39.4 ± 0.5
MOLT-4	CTL	100.0 ± 0.0	100.0 ± 0.0	100.0 ± 0.0
	PRT 1 µM	104.5 ± 2.4	120.8 ± 10.9	68.4 ± 6.6 *
	PRT 7.5 µM	139.6 ± 7.3 **	170.9 ± 11.8 ***	52.3 ± 9.3 **
RAJI	CTL	100.0 ± 0.0	100.0 ± 0.0	100.0 ± 0.0
	PRT 1 µM	105.3 ± 2.8	101.5 ± 3.6	69.2 ± 7.3
	PRT 15 µM	133.0 ± 9.9 *	107.6 ± 1.6	23.7 ± 1.4 **

Cells were incubated with PRT for 24 hours and the levels of superoxide anion, hydrogen peroxide and reduced glutathione were detected by flow cytometry using DHE, $DCFH_2DA$, and Mercury Orange probes, respectively, as described in the Materials and Methods section. The results are expressed as a percentage (%) normalized to control and represent the mean ± standard error of at least 2 independent assays. Statistical analysis was carried out by Kruskal-Wallis with Dunn's post-hoc test. *, p<0.05; **, p<.001; ***, p<0.001

3.9. Analysis of phosphorylated NF-kB levels by flow cytometry

To assess the efficacy of PRT in NF-kB pathway inhibition, the levels of the active form of NF-kB were analyzed using an anti-phosphorylated p65 monoclonal antibody.

As depitcted in Figure 17, PRT indeed is a NF-kB pathway inhibitor, since there was a dose-dependent decrease in phosphorylated p65 subunit levels in ALL cell lines [with higher concentrations there was a 1.46-, 1.61-, 1.77-, 2.16-, and 2.44-fold decrease in

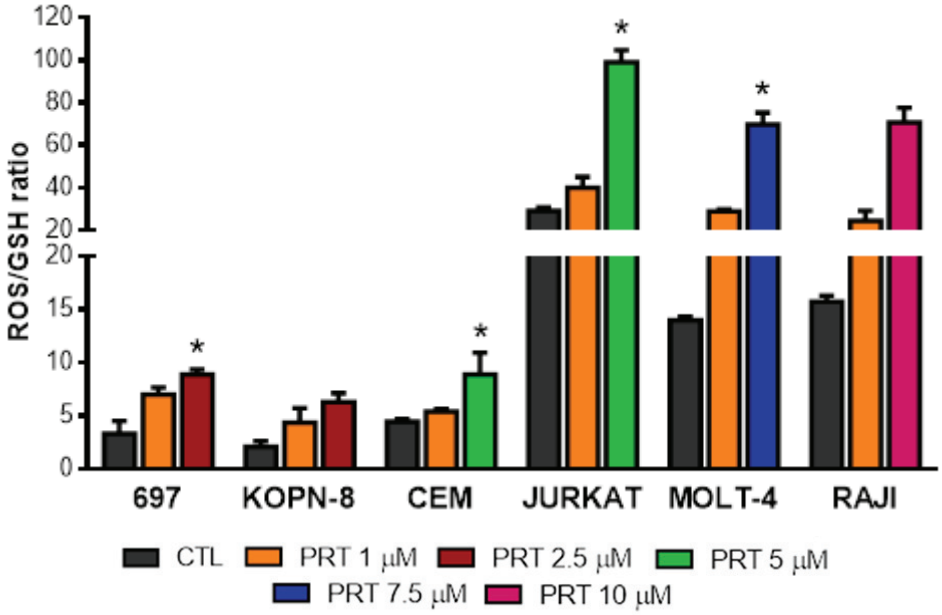

Figure 16 – Parthenolide's effect in oxidative stress levels in malignant hematological cell lines. Cells were incubated with PRT for 24 hours and oxidative stress was analyzed using specific probes as described in the Materials and Methods section. The results are expressed as the ratio between the mean fluorescence intensity of reactive oxygen species (ROS) and reduced glutathione (GSH) and represent the mean ± standard error of at least 2 independent experiments. Statistical analysis was carried out by Kruskal-Wallis with Dunn's post-hoc test. *, $p<0.05$

JURKAT (p=0.015), KOPN-8, 697, MOLT-4 (p=0.033), and CEM (p=0.027) cells respectively]. Regarding BL, phosphorylated p65 inhibition seemed not to be the main cause of apoptotic death induction. Another thing to note is that the basal levels of phosphorylated p65 were cell line and disease dependent, having T-ALL cell lines (JURKAT and MOLT-4) a higher activation of NF-kB pathway (Figure 17).

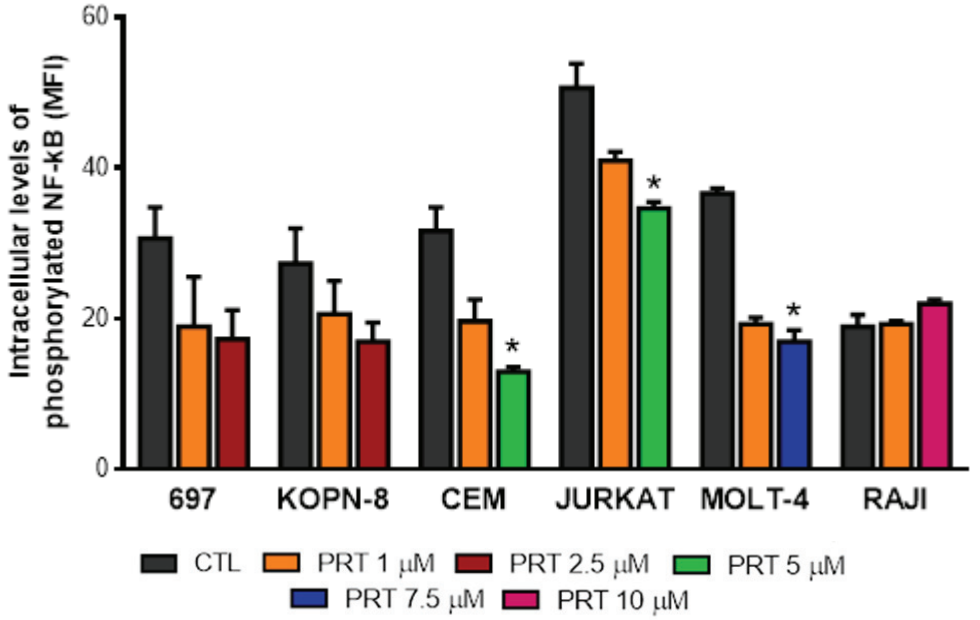

Figure 17 – Phosphorylated NF-kB levels in malignant hematological cell lines incubated in the absence (control) and presence of Parthenolide. Cells were incubated with PRT for 24 hours and the levels of phosphorylated NF-kB were analyzed using an anti-p65 subunit monoclonal antibody as described in the Materials and Methods section. The results are expressed as mean fluorescence intensity of p65 subunit and represent the mean ± standard error of 3 independent experiments. Statistical analysis was carried out by Kruskal-Wallis with Dunn's post-hoc test. *, $p<0.05$

Discussion

4. Discussion

4.1. Evaluation of the therapeutic potential of a NF-kB inhibitor in acute lymphoblastic leukemia and Burkitt lymphoma cell lines

Despite being very heterogeneous in terms of etiology, immunophenotype, cytogenetics, and clinical features, BL and the distinct subtypes of ALL share a relatively low/intermediate response rate to conventional chemotherapy regimens and are frequently associated with chemoresistance, considerable (long-term) toxicity and/or relapse. Therefore, it is of great importance to explore alternative areas of therapeutic intervention.

Playing an important role in the regulation of diverse biological processes such as cell proliferation and survival, NF-kB signaling has been appointed as one important player in all stages of tumorigenesis. Considering the well-established NF-kB cancer relations, PRT has been appointed as a valid option for cancer therapy improvement since several *in vitro* studies have demonstrated its antineoplastic activity in a wide range of solid and hematological neoplasms[44, 47, 54, 73–76, 85,86,120–131].

As such, this project aimed to clarify the therapeutic potential of PRT in cellular *in vitro* models of ALL and BL and to characterize the type of cell death induced and its molecular mechanisms.

The results indicate that PRT induced a time, dose and cell line dependent reduction on the metabolic activity of ALL and BL cell lines. After a 24 hour incubation period, RAJI cells were particularly susceptible to the compound since a smaller concentration of PRT was required to induce a 50% reduction in its metabolic activity at this timepoint. The IC_{50} for CEM, KOPN-8, 697, and MOLT-4 cells was also reached following a 24 hour incubation period. However, these cell lines required a higher dose of PRT. JURKAT cells seemed to be the less sensitive ones, with the IC_{50} being reached only after 48 hours of incubation. Nevertheless, after 72 hours of incubation, the cell line's sensitivity was somewhat different (time effect) with KOPN-8 cells behaving as the most sensitive ones. These results may be related with the cell type and genetic background. Another thing

to consider is the stage of the disease which the various cell lines represent, since the cell lines established at the time of diagnosis (KOPN-8, RAJI, and CEM) are more sensitive to PRT than the ones established after a relapse (697, MOLT-4, and JURKAT). For this reason, it may be interesting to evaluate copy-numbers variation of multidrug resistance gene (*MDR1*), which is usually amplified in some cell lines[132,133], as well as to analyze intrinsic or acquired expression of some proteins related with multidrug resistance, namely P-glycoprotein (P-gp), an ATP-dependent efflux pump, codified by the *MDR1* gene, that extrudes a variety of cytotoxic compounds out of the cells[132,133], and other ATP-binding cassette (ABC) transporters[132,134], major players in decreased intracellular drug accumulation and consequent clinical resistance to therapy[133].

In addition to the effect of PRT in single dose administration, we verified whether the daily administration of lower concentrations of the compound enhanced its effect, since this therapeutic regimen may potentiate metabolic activity reduction. In this case, there were no significant differences between the two therapeutic schemes. However, since the results were similar, daily administration may remain a possibility to be used as it enables a reduction in dose related toxicity complications. On the other hand, it is important to note that the drug delivery system does not mimic everything that happens in the human organism, being necessary a transposition of the study to a more complex model that considers PRT's pharmacokinetics and pharmacodynamics. Besides that, since NF-kB pathway is appointed as one of the reasons for chemo- and radiotherapy resistance (current therapies promote its activation), it would be interesting to perform association studies, evaluating its effect on current therapeutic regimens[78,135–139].

Many studies indicate that PRT induces a cytotoxic effect, promoting tumor cell death in different malignancies[47, 54, 74–76, 79, 85,86, 121–129, 131,140–146]. Regarding ALL and BL, our results revealed that PRT's reduction in metabolic activity was mainly related to programmed cell death activation, since the treatment led to blebbing, nuclear fragmentation, and apoptotic bodies' formation, some of the typical morphological features of apoptosis[147]. These characteristics are in accordance with annexin-V/7-AAD analysis where a significant decrease in cellular viability associated with a parallel increase in the number of cells in early stages of apoptosis was observed. Sub-G_1 peak

presence revealed by cell cycle analysis and the increased levels of cleaved caspase-3, also confirmed PRT-mediated apoptosis as a result of extrinsic and/or intrinsic pathways activation.

The upregulation of FAS and/or its ligand in B-ALL, BL, and one of T-ALL (MOLT-4) cell lines following PRT treatment, highlighted the possible involvement of the extrinsic apoptotic pathway, which, upon FAS-L stimulation and cross-linking of FAS and recruitment of FAS-associated death domain (FADD), drive to the assembly of the death-inducing signaling complex (DISC) together with procaspase-8 and -10. This results in caspase-8 activation, which triggers the execution of apoptosis by direct activation of other members of caspase family, such as caspase-3, -6, and -7, or starts a feedback loop that activates the intrinsic pathway, increasing the release of pro-apoptotic factors from mitochondria[148–150]. Regarding CEM and JURKAT cell lines, there were no changes in the levels of FAS and FAS-L suggesting that extrinsic-mediated apoptosis is not a relevant mechanism mediating the effect of PRT in this cell lines. However, it may be important to evaluate the levels of other tumor necrosis factor family members [e.g. TNF-related apoptosis-inducing ligand receptors 1 (TRAIL-R1) and 2 (TRAIL-R2), and TNF receptor (TNFR1 or TNFRSF1A)] to see if there is extrinsic pathway activation through a distinctive mechanism. Indeed, it has been suggested that CEM cells have increased expression of pro-apoptotic receptors, like TRAIL-R1 and TRAIL-R2, and decreased expression of anti-apoptotic ones, TRAIL-R3 and TRAIL-R4[151,152]. Besides that, studies in oral cancer claim that PRT increases TRAIL-R1 expression[128], appointing to a relevant connection between PRT treatment and extrinsic apoptosis. In JURKAT cells, according to Li-Weber and collaborators, apoptosis cannot be the result of death-receptor mediated pathways, since they have deficient FADD protein adaptors[153]. As such, this may be a mechanism responsible for greater resistance to PRT induced cytotoxicity.

On the other hand, intrinsic pathway of apoptosis is mainly related with intracellular sensed stimuli (cytokine deprivation, DNA damage, and endoplasmic reticulum stress) that engage BAX and BAK activity (with decreased levels of anti-apoptotic BCL-2 family proteins), converging in dissipation of mitochondrial membrane potential, mitochondrial outer membrane permeabilization, and cytosolic release of cytochrome

c[154]. This pro-apoptotic molecule triggers apoptosome assembly, activating caspase-9, which in turn activates caspase-3 and -7 leading to apoptosis. As such, JC-1 analysis results evidenced the involvement of this mitochondrial-mediated apoptotic pathway in all cell lines, since PRT treatment increased the disruption of mitochondria. These results are in concordance with other studies in ALL[74,75], BL[47], acute myeloblastic leukemia[122], promyelocytic leukemia[126], multiple myeloma[54], hepatocellular carcinoma[127,153], oral[128], colorectal[131,141], pancreatic[130], lung[129], ovarian[125], cervical, and breast[121,124] cancer cell lines, demonstrating that PRT is able to induce apoptotic cell death through intrinsic apoptosis, with BID, BCL-2, BCL-xL, and survivin (suppresses apoptosis by caspase-3 inhibition) downregulation, as well as BAX, cytochrome c, and caspase-9 upregulation.

Another mechanism to consider in PRT-mediated cytotoxicity is oxidative stress promotion. Our results report that PRT induced oxidative stress due to an increase in ROS (superoxide anion and/or hydrogen peroxide) with an associated decrease in GSH levels. Once again, our results seem to be in accordance with the available literature that proposes that PRT treatment increases the generation of ROS by upregulating superoxide production through NADPH oxidase activation and downregulating antioxidant defenses through covalent interaction with thiol groups (thioredoxin) and by targeting enzymatic components of glutathione pathway [glutamate-cysteine ligase catalytic subunit (GCLC) and glutathione peroxidase-1 (GPX1)][74, 76, 83, 85,86, 146,155,156]. Then, the exacerbated levels of oxidative stress are no longer favorable to tumor survival and have a deleterious effect on cancer cells. Indeed, this increase of ROS acts upon mitochondria causing disruption of its membrane potential and activation of apoptosis[47, 74–76, 83, 86, 124,125, 131, 146,155,156] through peroxynitrite irreversible inhibition of the electron transport complexes I, II, and III[74] and/or activation of c-Jun NH_2-terminal kinase (JNK) pathway[83,86] promoting mitochondrial release of cytochrome c through BCL-2 inhibition[76,122]. Besides this, PRT-mediated oxidative stress has been implicated in the accumulation of misfolded proteins in endoplasmic reticulum, triggering the death arm of unfolded protein response, amplifying apoptotic signaling[129,145].

More recently, PRT treatment has been appointed as an inducer of autophagy, a physiological process of organelles and macromolecules turnover, and nutrients

recycling, which involves the engulfment of cytoplasmic material and intracellular organelles with double-membrane vesicles (autophagosomes) that then fuse with lysosomes to form an autolysosome, where the captured material is degraded[157]. In fact, some studies in multiple myeloma[54], promyelocytic leukemia[126], osteosarcoma[158], cervical[124], breast[86], and pancreatic cancers[130] note that PRT administration induces an increase in the levels of some well-known autophagic proteins like BECLIN-1, autophagy-related protein (ATG) 3 and 5, p62, and microtubule-associated protein 1A/1B-light chain 3-II (LC3-II)[83]. Some of these authors also propose that PRT-mediated autophagy has an uncommon associated role (less cytoprotective), helping to induce apoptosis, since autophagy inhibition blocked PRT-induced apoptosis in pancreatic cancer cells[130]. Indeed, autophagosomes or ATG proteins may participate in lethal signaling at some specific situations: autophagosomes can act as platforms for caspase-8 activation or mediate selective autophagy of anti-apoptotic proteins [inhibitor of apoptosis proteins (IAPs)]; and ATG12 can directly interact with the anti-apoptotic BCL-2 protein, inhibiting its function and increasing apoptosis[157,159]. Lan and collaborators, based on their studies in promyelocytic leukemia, proposed that the increase in oxidative stress mediated by PRT promotes 4E-BP1 downregulation, which consequently leads to mammalian target of rapamycin complex 1 (mTORC1) release of ULK-1-ATG13-FIP200 and favors the formation of autophagosomes that, then, potentiate the induction of apoptosis[126]. Being an area of knowledge that is still under development and since morphological analysis depicts cytoplasmic vacuolization, it would be important to assess the possible autophagic relation between PRT, apoptosis, and oxidative stress, evaluating the levels of specific autophagic proteins and analyzing the formation of autolysosomes with monodansylcadaverine (MDC) and acridine orange staining[86, 124,127].

Besides having a cytotoxic effect in several cancer cells, PRT seems to have an anti-proliferative effect inducing cell cycle arrest in a cell line and disease dependent manner. In A549 and H1792 cells, lung cancer cell lines, was detected a cell cycle arrest in G_0/G_1 and G_2/M, respectively[129]. PRT also exhibited a significant cell cycle arrest at S and G_0/G_1 phases in HaCaT and A375 skin cancer cell lines[123]. Similarly, Guang and Xie, and Liu and collaborators demonstrated its potential to arrest cell cycle at G_1 phase in 5637 bladder

as well as in Panc-1 and BxPC3 pancreatic cancer cells by modulating cyclin D1 and phosphorylated cyclin-dependent kinase 2[123,130]. In SEM and RS4;11 B-ALL cells, PRT induced growth arrest at S to G_2/M transition[75]. In a first analysis, our results revealed that PRT did not have a relevant effect on cell cycle progression, being JURKAT and MOLT-4 the only cell lines that evidenced a cell cycle arrest in G_1 and G_2/M, respectively. However, after treatment with increasing concentrations of PRT, KOPN-8 cells revealed a tendency to accumulate in G_0/G_1 phase, which suggests that PRT had some effect in checkpoint regulators that participate in transition of G_1 to S phase. As a matter of fact, cyclin D has been tightly associated with NF-kB pathway stimulation, since its gene expression is regulated by NF-kB transcription factor[42, 56–59,147]. PRT seems to induce CEM's cell cycle arrest by a mechanism very similar to MOLT-4 cells. On the other hand, contrary to what is observed in the literature (PRT's administration increases G_0/G_1 cell population while decreasing the number of S phase cells[47]), PRT's effect in RAJI cell line was not clear. This may be related with *c-MYC* upregulation (resultant from *MYC-IGH* translocation), leading to an increase in proliferation and growth rate[160,161] [c-MYC activates cyclin D2 and cyclin D3, promoting the G_1-S phase transition[160,161]; c-MYC regulates various microRNAs (miRs) like miR34 and miR29a targeting TP53 and cyclin-dependent kinase 6 (CDK6) (G_1/S checkpoint controllers), respectively[161]]. Besides that, EBV latent infection can have an impact on cell cycle progression (G_2/M restriction point), inducing a higher propensity for mitotic arrest (and polyploid induction, leading to increase apoptotic resistance)[162]. In addition, this may be due to the fact that cells undergoing apoptosis were, initially, at a later stage of the cell cycle (G_2/M) and, after DNA fragmentation, are counted as being in G_1 phase instead of appearing at the sub-G_1 peak[117]. PRT treatment seemed to have no effect on the cell cycle of 697 cells. This may be consequence of the expression of E2A-PBX specific truncated protein, which induces a downregulation in some cell cycle suppressor proteins like CDKN2A, $p14^{ARF}$ (p53 activator) and $p16^{INK4A}$ [inhibits retinoblastoma (Rb) phosphorylation], conferring not only a superior proliferative capacity (it possesses upregulation of *c-MYC* as well) but also an ability to circumvent various cell cycle checkpoints[163,164]. Taking these results into account, it would be important to analyze the levels of various proteins involved in

cell cycle progression and control, such as cyclins, CDKs, CDK inhibitors, and other cell cycle suppressor proteins.

To assess the inhibition of IKK by PRT, the expression of the active form of NF-kB (p65 subunit) was analyzed. The observed decrease in NF-kB levels in ALL *in vitro* models is indicative of PRT involvement in IKK inhibition, allowing IkB to remain bounded to NF-kB allowing its sequestering in the cytoplasm. In addition, PRT also inhibits the NF-kB pathway through its direct interaction with activated NF-kB, preventing its interaction with the DNA and the consequent transcription of the several genes it regulates. Therefore, it would be interesting to analyze, by chromatin immunoprecipitation assays, what happened at that level, checking if the downstream inhibition of the pathway would be much more evident than the results depicted. Indeed, this may be the predominant mechanism of action in RAJI cell line (dependent of NF-kB inhibition), since FC results showed a slight increase in phosphorylated NF-kB levels. Besides this, it is noteworthy that what was being evaluated was the canonical p65 subunit levels (RelA), not knowing whether PRT's administration also affected the non-canonical pathway. Supposedly, non-canonical pathway should not be affected since PRT's inhibition effect is at the level of IKKβ and p65, two proteins that only belong to the canonical pathway[45–47, 52, 54, 58, 68–70, 80–82,165]. As such, it would be interesting to evaluate the levels of RelB or p52, since this could be one of the explanations for the different sensitivities to PRT. In fact, the constitutive active NOTCH1 protein in T-ALL cell lines, mainly in CEM and JURKAT, positively regulates the expression of RelB and activates the IKK promoting the expression of proliferative and survival/apoptotic genes[142,143]. Moreover, especially in the case of the BL model, there may be other mechanisms to consider and scrutinize. One of these is an atypical NF-kB signaling pathway activated upon oxidative stress stimulation[166–168]. This IKK independent activation of p65 (relies on IkBα phosphorylation by tyrosine kinases and its dissociation from p65)[166–168] can result from PRT induction of oxidative stress and be a mechanism associated with lower sensitivity to NF-kB inhibition in RAJI cell line, being a viable explanation for the detected increase in p65 levels upon treatment with the compound.

Conclusion

5. Conclusion

The main conclusions of this dissertation focused on the evaluation of Parthenolide's therapeutic potential in several *in vitro* models of acute lymphoblastic leukemia and Burkitt lymphoma were:

⇒ PRT administration in *in vitro* models of lymphoid malignancies reduced cellular metabolic activity in dose, time and cell line dependent manner;

⇒ Single and daily administration schemes gave similar results. As such, daily administration may remain a possibility as it may enable a reduction in dose related toxicity complications;

⇒ IKKβ inhibition leads to the activation of caspase-dependent apoptosis in all cell lines;

⇒ Extrinsic apoptotic pathway through FAS/FAS-L interaction was mainly involved in 697 and MOLT-4 cell death;

⇒ PRT administration induced oxidative stress due to an increase in superoxide anion and/or hydrogen peroxide with an associated decrease in GSH levels;

⇒ Deleterious levels of reactive oxygen species lead to intrinsic apoptotic pathway in ALL cell lines, being the cause or consequence of mitochondrial membrane potential disruption;

⇒ Cell cycle progression was not equally affected in all cell lines, being JURKAT and MOLT-4 the only cell lines that had an evident G_1 and G_2/M cell cycle arrest, respectively.

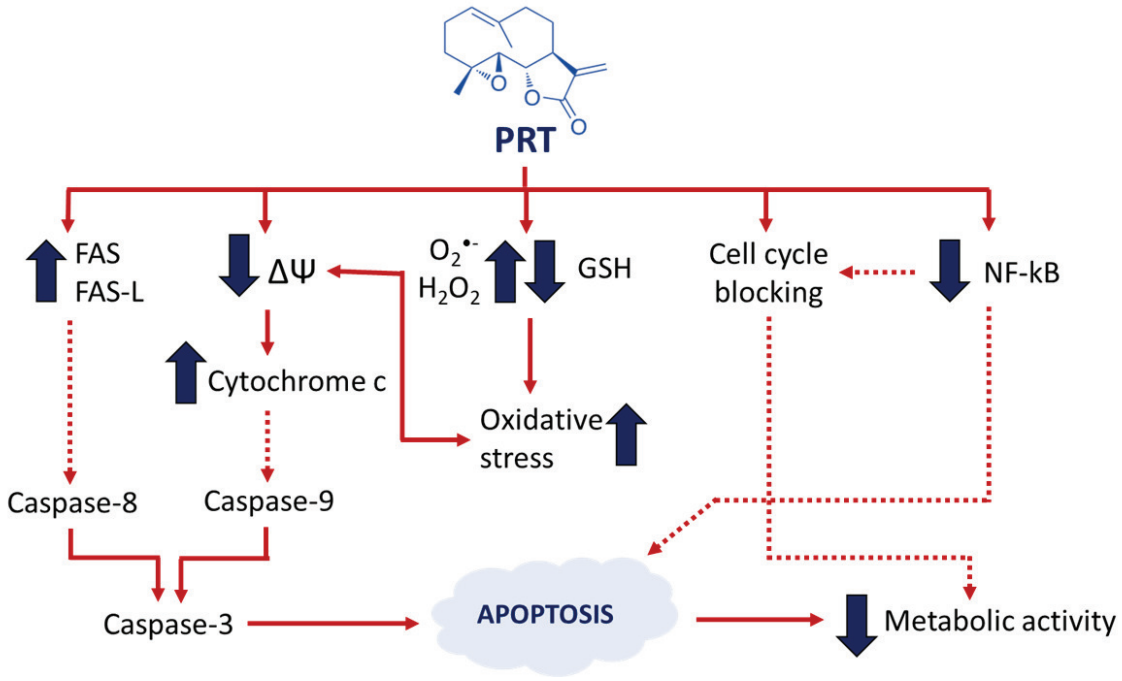

Figure 18 – Schematic representation of Parthenolide's effects on acute lymphoblastic leukemia and Burkitt lymphoma cell lines.

In conclusion, the wide range of effects demonstrated by these results, suggest that Parthenolide may constitute a valid therapeutic approach in B cell derived ALL and BL, as well as in T-ALL at diagnosis.

To further confirm this potential, it is proposed to evaluate the possibility of associating Parthenolide with conventional chemotherapeutic regimens and/or to assess its therapeutic potential in primaty cultures established from ALL and BL patient's blood samples.

References

6. References

1. Rieger, M. & Schroeder, T. Hematopoiesis. *Cold Spring Harb Perspect Biol* **4,** (2012).
2. Robb, L. Cytokine receptors and hematopoietic differentiation. *Oncogene* **26,** 6715–23 (2007).
3. Dalerba, P., Cho, R. & Clarke, M. Cancer Stem Cells: Models and Concepts. *Annu Rev Med* **58,** 267–284 (2007).
4. Myatt, S. & Lam, E. Promiscuous and lineage-specific roles of cell cycle regulators in haematopoiesis. *Cell Div* **2,** 6 (2007).
5. Orkin, S. & Zon, L. Hematopoiesis: An Evolving Paradigm for Stem Cell Biology. *Cell* **132,** 631–44 (2008).
6. Hoffbrand, A. & Moss, P. *Hoffbrand's Essential Haematology*. (Wiley-Blackwell, 2016).
7. Hoffbrand, A., Higgs, D., Keeling, D. & Mehta, A. *Postgraduate Haematology*. (Wiley-Blackwell, 2016).
8. Ho, M., Medcalf, R., Livesey, S. & Traianedes, K. The dynamics of adult haematopoiesis in the bone and bone marrow environment. *Br J Haematol* **170,** 472–86 (2015).
9. Lobo, N., Shimono, Y., Qian, D. & Clarke, M. The Biology of Cancer Stem Cells. *Annu Rev Cell Dev Biol* **23,** 675–99 (2007).
10. Seeley, R. R., Stephens, T. D. & Tate, P. *Anatomy & Phisiology*. (McGraw-Hill, 2008).
11. Wadhwa, M. & Thorpe, R. Haematopoietic growth factors and their therapeutic use. *Thromb Haemost* **99,** 863–73 (2008).
12. Kaushansky, K., Lichtman, M. A., Prchal, J. T., Levi, M., Press, O. W., Burns, L. J., Caligiuri, M. A. & Williams, W. J. *Williams Hematology*. (McGraw-Hill Education, 2016).
13. Chao, M., Seita, J. & Weissman, I. Establishment of a Normal Hematopoietic and Leukemia Stem Cell Hierarchy. *Cold Spring Harb Symp Quant Biol* **73,** 439–449 (2008).
14. Hystad, M., Myklebust, J. H., Bø, T. H., Sivertsen, E. A., Rian, E., Forfang, L., Munthe, E., Rosenwald, A., Chiorazzi, M., Jonassen, I., Staudt, L. M. & Smeland, E. B. Characterization of early stages of human B cell development by gene expression profiling. *J Immunol* **179,** 3662–71 (2007).
15. Murphy, K. *Janeway's Immunobiology*. (Garland Science, 2012).
16. Longo, D. L., Fauci, A., Kasper, D., Hauser, S., Jameson, J. L. & Loscalzo, J. *Harrison's Principles of Internal Medicine*. (McGraw-Hill Education, 2012).
17. Shaffer, A. L., Rosenwald, A. & Staudt, L. M. Lymphoid Malignancies: the dark side of B-cell differentiation. *Nat Rev Immunol* **2,** 920–32 (2002).
18. Dalla-Favera, R. Lymphoid malignancies: many tumor types, many altered genes, many therapeutic challenges. *J Clin Invest* **122,** 3396–7 (2012).
19. Onciu, M. Acute Lymphoblastic Leukemia. *Hematol. Oncol. Clin. North Am.* **23,** 655–674 (2009).
20. Stewart, B. W. & Wild, C. P. *World Cancer Report 2014*. (World Health Organization, 2014).
21. Heilmeyer, L. & Begemann, H. *Atlas of Clinical Hematology*. (Springer, 2004).
22. Beutler, E., Lichtman, M. A., Coller, B. S. & Kipps, T. J. *Williams Hematology*. (McGraw-Hill, 1995).
23. Bunn, H. F. & Aster, J. C. *Pathophysiology of Blood Disorders*. (McGraw-Hill Education, 2011).

24. Inaba, H., Greaves, M. & Mullighan, C. G. Acute lymphoblastic leukaemia. *Lancet* **381,** 1943–1955 (2013).
25. Dias, A., Kenderian, S. J., Westin, G. F. & Litzow, M. R. Novel Therapeutic Strategies in Acute Lymphoblastic Leukemia. *Curr. Hematol. Malig. Rep.* **11,** 253–264 (2016).
26. Hunger, S. P. & Mullighan, C. G. Acute Lymphoblastic Leukemia in Children. *N Engl J Med* **373,** 1541–1552 (2015).
27. Pui, C.-H., Robison, L. L. & Look, A. T. Acute lymphoblastic leukaemia. *Lancet* **371,** 1030–1043 (2008).
28. Layton Tovar, C. F. & Mendieta Zerón, H. Intracellular Signaling Pathways Involved in Childhood Acute Lymphoblastic Leukemia; Molecular Targets. *Indian J Hematol Blood Transfus* **32,** 141–53 (2016).
29. Pui, C.-H., Relling, M. V. & Downing, J. R. Acute Lymphoblastic Leukemia. *N Engl J Med* **350,** 1535–1548 (2004).
30. Durinck, K., Goossens, S., Peirs, S., Wallaert, A., Van Loocke, W., Matthijssens, F., Pieters, T., Milani, G., Lammens, T., Rondou, P., Van Roy, N., Benoit, Y., Haigh, J., Speleman, F., Poppe, B. & Van Vlierberghe, P. Novel biological insights in T-cell acute lymphoblastic leukemia. *Exp. Hematol.* **43,** 625–39 (2015).
31. Casulo, C. & Friedberg, J. Treating Burkitt Lymphoma in Adults. *Curr. Hematol. Malig. Rep.* **10,** 266–271 (2015).
32. Schmitz, R., Ceribelli, M., Pittaluga, S., Wright, G. & Staudt, L. M. Oncogenic mechanisms in Burkitt lymphoma. *Cold Spring Harb. Perspect. Med.* **4,** (2014).
33. Dave, S. S., Fu, K., Wright, G. W., Lam, L. T., Kluin, P., Boerma, E.-J., Greiner, T.C., Weisenburger, D. D., Rosenwald, A., Ott, G., Müller-Hermelink, H.-K., Gascoyne, R. D., Delabie, J., Rimsza, L. M., Braziel, R. M., Grogan, T. M., Campo, E., Jaffe, E. S., Dave, B. J., Sanger, W., Bast, M., Vose, J. M., Armitage, J. O., Connors, J .M., Smeland, E. B., Kvaloy, S., Holte, H., Fisher, R. I., Miller, T. P., Montserrat, E., Wilson, W. H., Bahl, M., Zhao, H., Yang, L., Powell, J., Simon, R., Chan, W. C. & Staudt, L. M. Molecular Diagnosis of Burkitt's Lymphoma. *N Engl J Med* **354,** 2431–2442 (2006).
34. Grywalska, E., Markowicz, J., Grabarczyk, P., Pasiarski, M. & Roliński, J. Epstein-Barr virus-associated lymphoproliferative disorders. *Postep. Hig Med Dosw* **67,** 481–90 (2013).
35. Said, J., Lones, M. & Yea, S. Burkitt lymphoma and MYC: what else is new? *Adv Anat Pathol* **21,** 160–5 (2014).
36. Kimura, H., Kawada, J. & Ito, Y. Epstein-Barr virus-associated lymphoid malignancies: the expanding spectrum of hematopoietic neoplasms. *Nagoya J. Med. Sci.* **75,** 169–79 (2013).
37. Thorley-Lawson, D. A. & Allday, M. J. The curious case of the tumour virus: 50 years of Burkitt's lymphoma. *Nat. Rev. Microbiol.* **6,** 913–924 (2008).
38. Thorley-Lawson, D. A. Epstein-Barr virus: exploiting the immune system. *Nat. Rev. Immunol.* **1,** 75–82 (2001).
39. Owen, J. A., Punt, J. & Stranford, S. A. *Kuby Immunology*. (W.H. Freeman and Company, 2009).
40. Xiao, G. & Fu, J. NF-κB and cancer: a paradigm of Yin-Yang. *Am. J. Cancer Res.* **1,** 192–221 (2011).
41. Braun, T., Carvalho, G., Fabre, C., Grosjean, J., Fenaux, P. & Kroemer, G. Targeting NF-κB in hematologic malignancies. *Cell Death Differ.* **13,** 748–758 (2006).
42. Jost, P. J. & Ruland, J. Aberrant NF-kB signaling in lymphoma: mechanisms, consequences, and therapeutic implications. *Blood* **109,** 2700–7 (2007).
43. Sun, X.-F. & Zhang, H. NFKB and NFKBI polymorphisms in relation to susceptibility of

tumour and other diseases. *Histol Histopathol* **22,** 1387–98 (2007).

44. Varga, G., Mikala, G., Andrikovics, H., Koszarska, M., Balassa, K., Ádám, E., Kozma, A., Tordai, A. & Masszi, T. NFKB1 -94ins/delATTG polymorphism is a novel prognostic marker in first line-treated multiple myeloma. *Br J Haematol* **168,** 679–88 (2015).
45. Pajak, B., Gajkowska, B. & Orzechowski, A. Molecular basis of parthenolide-dependent proapoptotic activity in cancer cells. *Folia Histochem Cytobiol* **46,** 129–35 (2008).
46. Amorim, M. H. R., Gil da Costa, R. M., Lopes, C. & Bastos, M. M. S. M. Sesquiterpene lactones: adverse health effects and toxicity mechanisms. *Crit Rev Toxicol* **43,** 559–79 (2013).
47. Li, Y., Zhang, Y., Fu, M., Yao, Q., Zhuo, H., Lu, Q., Niu, X., Zhang, P., Pei, Y. & Zhang, K. Parthenolide induces apoptosis and lytic cytotoxicity in Epstein-Barr virus-positive Burkitt lymphoma. *Mol Med Rep* **6,** 477–82 (2012).
48. Liu, S.-F., Wang, H., Lin, X.-C., Xiang, H., Deng, X.-Y., Li, W., Tang, M. & Cao, Y. NF-kappaB inhibitors induce lytic cytotoxicity in Epstein-Barr virus-positive nasopharyngeal carcinoma cells. *Cell Biol Int* **32,** 1006–13 (2008).
49. Demchenko, Y. N., Brents, L. A., Li, Z., Bergsagel, L. P., McGee, L. R. & Kuehl, M. W. Novel inhibitors are cytotoxic for myeloma cells with NFkB inducing kinase-dependent activation of NFkB. *Oncotarget* **5,** 4554–66 (2014).
50. Inoue, J., Gohda, J., Akiyama, T. & Semba, K. NF-κB activation in development and progression of cancer. *Cancer Sci.* **98,** 268–274 (2007).
51. Ramakrishnan, V. & D'Souza, A. Signaling Pathways and Emerging Therapies in Multiple Myeloma. *Curr Hematol Malig Rep* **11,** 156–64 (2016).
52. Kong, F.-C., Zhang, J.-Q., Zeng, C., Chen, W.-L., Ren, W.-X., Yan, G.-X., Wang, H.-X., Li, Q.-B. & Chen, Z.-C. Inhibitory effects of parthenolide on the activity of NF-κB in multiple myeloma via targeting TRAF6. *J Huazhong Univ Sci Technol. Med Sci* **35,** 343–9 (2015).
53. Demchenko, Y. N. & Kuehl, W. M. A critical role for the NFkB pathway in multiple myeloma. *Oncotarget* **1,** 59–68 (2010).
54. Suvannasankha, A., Crean, C. D., Shanmugam, R., Farag, S. S., Abonour, R., Boswell, H. S. & Nakshatri, H. Antimyeloma effects of a sesquiterpene lactone parthenolide. *Clin Cancer Res* **14,** 1814–22 (2008).
55. Valko, M., Leibfritz, D., Moncol, J., Cronin, M. T. D., Mazur, M. & Telser, J. Free radicals and antioxidants in normal physiological functions and human disease. *Int J Biochem Cell Biol* **39,** 44–84 (2007).
56. Aggarwal, B. Nuclear factor-κB: the enemy within. *Cancer Cell* **6,** 203–8 (2004).
57. Bharti, A. & Aggarwal, B. Nuclear factor-kappa B and cancer: its role in prevention and therapy. *Biochem Pharmacol* **64,** 883–8 (2002).
58. Durand, J. & Baldwin, A. Targeting IKK and NF-κB for Therapy. *Adv Protein Chem Struct. Biol* **107,** 77–115 (2017).
59. Gupta, S., Sundaram, C., Reuter, S. & Aggarwal, B. Inhibiting NF-κB activation by small molecules as a therapeutic strategy. *Biochim Biophys Acta* **1799,** 775–787 (2010).
60. Olivier, S., Robe, P. & Bours, V. Can NF-κB be a target for novel and efficient anti-cancer agents? *Biochem Pharmacol* **72,** 1054–68 (2006).
61. Chesi, M. & Bergsagel, P. L. Advances in the pathogenesis and diagnosis of multiple myeloma. *Int J Lab Hematol* **37 Suppl 1,** 108–14 (2015).
62. Gunn, E. J., Williams, J. T., Huynh, D. T., Iannotti, M. J., Han, C., Barrios, F. J., Kendall, S., Glackin, C. A., Colby, D. A. & Kirshner, J. The natural products parthenolide and andrographolide exhibit anti-cancer stem cell activity in multiple myeloma. *Leuk*

Lymphoma **52,** 1085–97 (2011).

63. Chesi, M. & Bergsagel, P. L. Molecular pathogenesis of multiple myeloma: basic and clinical updates. *Int J Hematol* **97,** 313–23 (2013).
64. Naymagon, L. & Abdul-Hay, M. Novel agents in the treatment of multiple myeloma: a review about the future. *J. Hematol. Oncol.* **9,** 52 (2016).
65. Gao, M., Kong, Y., Yang, G., Gao, L., Shi, J., Gao, M., Kong, Y., Yang, G., Gao, L. & Shi, J. Multiple myeloma cancer stem cells. *Oncotarget* **7,** 35466–35477 (2016).
66. Rajkumar, S. V. & Kumar, S. Multiple Myeloma: Diagnosis and Treatment. *Mayo Clin. Proc.* **91,** 101–119 (2016).
67. Rajkumar, S. V. Myeloma today: Disease definitions and treatment advances. *Am J Hematol* **91,** 90–100 (2016).
68. Kreuger, M. R. O., Grootjans, S., Biavatti, M. W., Vandenabeele, P. & D'Herde, K. Sesquiterpene lactones as drugs with multiple targets in cancer treatment: focus on parthenolide. *Anticancer. Drugs* **23,** 883–96 (2012).
69. Mathema, V. B., Koh, Y.-S., Thakuri, B. C. & Sillanpää, M. Parthenolide, a Sesquiterpene Lactone, Expresses Multiple Anti-cancer and Anti-inflammatory Activities. *Inflammation* **35,** 560–565 (2012).
70. Ghantous, A., Sinjab, A., Herceg, Z. & Darwiche, N. Parthenolide: from plant shoots to cancer roots. *Drug Discov Today* **18,** 894–905 (2013).
71. Jordan, C. T. The leukemic stem cell. *Best Pr. Res Clin Haematol* **20,** 13–18 (2007).
72. Pei, S. & Jordan, C. T. How close are we to targeting the leukemia stem cell? *Best Pr. Res Clin Haematol* **25,** 415–418 (2012).
73. Diamanti, P., Cox, C. V, Moppett, J. P. & Blair, A. Parthenolide eliminates leukemia-initiating cell populations and improves survival in xenografts of childhood acute lymphoblastic leukemia. *Blood* **121,** 1384–93 (2013).
74. Zunino, S. J., Ducore, J. M. & Storms, D. H. Parthenolide induces significant apoptosis and production of reactive oxygen species in high-risk pre-B leukemia cells. *Cancer Lett* **254,** 119–27 (2007).
75. Zunino, S. J., Storms, D. H. & Ducore, J. M. Parthenolide treatment activates stress signaling proteins in high-risk acute lymphoblastic leukemia cells with chromosomal translocation t(4;11). *Int J Oncol* **37,** 1307–1313 (2010).
76. Wang, W., Adachi, M., Kawamura, R., Sakamoto, H., Hayashi, T., Ishida, T., Imai, K. & Shinomura, Y. Parthenolide-induced apoptosis in multiple myeloma cells involves reactive oxygen species generation and cell sensitivity depends on catalase activity. *Apoptosis* **11,** 2225–2235 (2006).
77. Kong, F., Chen, Z., Li, Q., Tian, X., Zhao, J., Yu, K., You, Y. & Zou, P. Inhibitory effects of parthenolide on the angiogenesis induced by human multiple myeloma cells and the mechanism. *J Huazhong Univ Sci Technol. Med Sci* **28,** 525–530 (2008).
78. Ferrucci, V., Boffa, I., De Masi, G. & Zollo, M. Natural compounds for pediatric cancer treatment. *Naunyn Schmiedebergs Arch Pharmacol* **389,** 131–49 (2016).
79. Nasim, S. & Crooks, P. A. *Antileukemic activity of aminoparthenolide analogs*. *Bioorg Med Chem Lett* **18,** (2008).
80. Li, F. & Sethi, G. Targeting transcription factor NF-kappaB to overcome chemoresistance and radioresistance in cancer therapy. *Biochim Biophys Acta* **1805,** 167–80 (2010).
81. McCreath, S. & Delgoda, R. Chemotherapeutics. in *Pharmacognosy : Fundamentals, Applications and Strategies* (Academic Press, 2016).
82. Hohmann, M., Longhi-Balbinot, D. T., Guazelli, C., Navarro, S. A., Zarpelon, A. C.,

Casagrande, R., Arakawa, N.S. & Verri Jr, W. A. Sesquiterpene Lactones: Structural Diversity and Perspectives as Anti-Inflammatory Molecules. in *Studies in Natural Products Chemistry, Volume 49* 243–264 (Elsevier, 2016).

83. Gali-Muhtasib, H., Hmadi, R., Kareh, M., Tohme, R. & Darwiche, N. Cell death mechanisms of plant-derived anticancer drugs: beyond apoptosis. *Apoptosis* **20,** 1531–62 (2015).
84. Taleghani, A., Nasseri, M. & Iranshahi, M. Synthesis of dual-action parthenolide prodrugs as potent anticancer agents. *Bioorg Chem* **71,** 128–134 (2017).
85. Pei, S., Minhajuddin, M., Callahan, K. P., Balys, M., Ashton, J. M., Neering, S. J., Lagadinou, E. D., Corbett, C., Ye, H., Liesveld, J. L., O'Dwyer, K. M., Li, Z., Shi, L., Greninger, P., Settleman, J., Benes, C., Hagen, F. K., Munger, J., Crooks, P. A., Becker, M. W. & Jordan, C. T. Targeting Aberrant Glutathione Metabolism to Eradicate Human Acute Myelogenous Leukemia Cells. *J Biol Chem* **288,** 33542–58 (2013).
86. D'Anneo, A., Carlisi, D., Lauricella, M., Puleio, R., Martinez, R., Di Bella, S., Di Marco, P., Emanuele, S., Di Fiori, R., Guercio, A., Vento, R. & Tesoriere, G. Parthenolide generates reactive oxygen species and autophagy in MDA-MB231 cells. A soluble parthenolide analogue inhibits tumour growth and metastasis in a xenograft model of breast cancer. *Cell Death Dis.* **4,** e891 (2013).
87. Findley, H. J., Cooper, M., Kim, T., Alvarado, C. & Ragab, A. Two new acute lymphoblastic leukemia cell lines with early B-cell phenotypes. *Blood* **60,** 1305–9 (1982).
88. Matsuo, Y. & Drexler, H. Establishment and characterization of human B cell precursor-leukemia cell lines. *Leuk Res* **22,** 567–79 (1998).
89. Foley, G. E., Lazarus, H., Farber, S., Uzman, B. G., Boone, B. A. & McCarthy, R. E. Continuous culture of Human Lymphoblasts from Peripheral Blood of a Child with Acute Leukemia. *Cancer* **18,** 522–9 (1965).
90. Schneider, U., Schwenk, H. & Bornkamm, G. Characterization of EBV-genome negative null and T cell lines derived from children with acute lymphoblastic leukemia and leukemic transformed non-Hodgkin lymphoma. *Int. J. Cancer* **19,** 621–6 (1977).
91. Rodrigues, N., Rowan, A., Smith, M. E., Kerr, I. B., Bodmer, W. F., Gannon, J. V. & Lane, D. P. p53 mutations in colorectal cancer. *Proc Natl Acad Sci U S A* **87,** 7555–9 (1990).
92. Greenberg, J. M., Gonzalez-Sarmiento, R., Arthur, D. C., Wilkowski, C. W., Streifel, B. J. & Kersey, J. H. Immunophenotypic and cytogenetic analysis of Molt-3 and Molt-4: human T-lymphoid cell lines with rearrangement of chromosome 7. *Blood* **72,** 1755–60 (1988).
93. Minowada, J., Onuma, T. & Moore, G. Rosette-forming human lymphoid cell lines. I. Establishment and evidence for origin of thymus-derived lymphocytes. *J Natl Cancer Inst.* **49,** 891–5 (1972).
94. Epstein, M. A., Achong, B. G., Barr, Y. M., Zajac, B., Henle, G. & Henle W. Morphological and virological investigations on cultured Burkitt tumor lymphoblasts (strain Raji). *J Natl Cancer Inst.* **37,** 547–59 (1966).
95. Rich, S., Bose, M., Tempst, P. & Rudofsky, U. Purification, microsequencing, and immunolocalization of p36, a new interferon-alpha-induced protein that is associated with human lupus inclusions. *J Biol Chem.* **271,** 1118–26 (1996).
96. Pulvertaft, J. Cytology of Burkitt's Tumour (African Lymphoma). *Lancet* **1,** 238–40 (1964).
97. Hamid, R., Rotshteyn, Y., Rabadi, L., Parikh, R. & Bullock, P. Comparison of alamar blue and MTT assays for high through-put screening. *Toxicol Vitr.* **18,** 703–10 (2004).
98. Riss, T. L., Moravec, R. A., Niles, A. L., Duellman, S., Benink, H. A., Worzella, T. J. & Minor, L. *Cell Viability Assays*. *Assay Guidance Manual* (2004).
99. Rampersad, S. Multiple Applications of Alamar Blue as an Indicator of Metabolic Function

and Cellular Health in Cell Viability Bioassays. *Sensors (Basel)* **12,** 12347–60 (2012).

100. Vega-Avila, E. & Pugsley, M. An overview of colorimetric assay methods used to assess survival or proliferation of mammalian cells. *Proc West Pharmacol Soc* **54,** 10–4 (2011).
101. O'Brien, J., Wilson, I., Orton, T. & Pognan, F. Investigation of the Alamar Blue (resazurin) fluorescent dye for the assessment of mammalian cell cytotoxicity. *Eur. J. Biochem.* **267,** 5421–5426 (2000).
102. Rieger, A. M., Nelson, K. L., Konowalchuk, J. D. & Barreda, D. R. Modified annexin V/propidium iodide apoptosis assay for accurate assessment of cell death. *J. Vis. Exp.* (2011).
103. Hingorani, R., Deng, J., Elia, J., McIntyre, C. & Mittar, D. Detection of Apoptosis Using the BD Annexin V FITC Assay on the BD FACSVerse™ System. (2011).
104. Lecoeur, H., Ledru, E., Prévost, M. & Gougeon, M. Strategies for phenotyping apoptotic peripheral human lymphocytes comparing ISNT, annexin-V and 7-AAD cytofluorometric staining methods. *J Immunol Methods* **209,** 111–23 (1997).
105. Zimmermann, M. & Meyer, N. Annexin V/7-AAD staining in Keratinocytes. in *Mammalian Cell Viability: Methods in Molecular Biology* (ed. Martin J. Stoddart) **740,** 57–63 (Humana Press, 2011).
106. Almeida, S., Sarmento-Ribeiro, A., Januário, C., Rego, A. & Oliveira, C. Evidence of apoptosis and mitochondrial abnormalities in peripheral blood cells of Huntington's disease patients. *Biochem Biophys Res Commun* **374,** 599–603 (2008).
107. Reers, M., Smiley, S. T., Mottola-Hartshorn, C., Chen, A., Lin, M. & Chen, L. B. Mitochondrial membrane potential monitored by JC-1 dye. *Methods Enzym.* **260,** 406–17 (1995).
108. Feng, Y., Wang, Y., Jiang, C., Fang, Z., Zhang, Z., Lin, X., Sun, L. & Jiang, W. Nicotinamide induces mitochondrial-mediated apoptosis through oxidative stress in human cervical cancer HeLa cells. *Life Sci* **181,** 62–69 (2017).
109. Chen, J., Rogers, S. C. & Kavdia, M. Analysis of kinetics of dihydroethidium fluorescence with superoxide using xanthine oxidase and hypoxanthine assay. *Ann. Biomed. Eng.* **41,** 327–37 (2013).
110. Owusu-Ansah, E., Yavari, A. & Banerjee, U. A protocol for in vivo detection of reactive oxygen species. *Protoc. Exch.* (2008).
111. Chen, X., Zhong, Z., Xu, Z., Chen, L. & Wang, Y. 2′,7′-Dichlorodihydrofluorescein as a fluorescent probe for reactive oxygen species measurement: Forty years of application and controversy. (2010).
112. du Plessis, L., Laubscher, P., Jooste, J., du Plessis, J., Franken, A., van Aarde, N. & Eloff, F. Flow Cytometric Analysis of the Oxidative Status in Human Peripheral Blood Mononuclear Cells of Workers Exposed to Welding Fumes. *J Occup Env. Hyg* **7,** 367–374 (2010).
113. Spyratos, F. DNA content and cell cycle analysis by flow cytometry in clinical samples: application in breast cancer. *Biol Cell* **78,** 69–72 (1993).
114. Krishan, A. Rapid flow cytofluorometric analysis of mammalian cell cycle by propidium iodide staining. *J Cell Biol* **66,** 188–93 (1975).
115. Pozarowski, P. & Darzynkiewicz, Z. Analysis of Cell Cycle by Flow Cytometry. in *Checkpoint Controls and Cancer* (ed. Schönthal, A.) **281,** 301–311 (Humana Press, 2004).
116. Rabinovitch, P. DNA content histogram and cell-cycle analysis. in *Flow Cytometry: Methods in Cell Biology* (eds. Darzynkiewicz, Z., Robinson, J. & Crissman, H.) **41,** 263–96 (Academic Press, 1994).

117. Wlodkowic, D., Telford, W., Skommer, J. & Darzynkiewicz, Z. Apoptosis and beyond: cytometry in studies of programmed cell death. *Methods Cell Biol.* **103,** 55–98 (2011).
118. Collins, J., Schandl, C., Young, K., Vesely, J. & Willingham, M. Major DNA Fragmentation Is a Late Event in Apoptosis. *J Histochem. Cytochem* **45,** 923–34 (1997).
119. Chan, A., Reiter, R., Wiese, S., Fertig, G. & Gold, R. Plasma membrane phospholipid asymmetry precedes DNA fragmentation in different apoptotic cell models. *Histochem Cell Biol* **110,** 553–8 (1998).
120. Nasim, S. & Crooks, P. Antileukemic activity of aminoparthenolide analogs. *Bioorg Med Chem Lett* **18,** 3870–3 (2008).
121. Al-Fatlawi, A. A., Al-Fatlawi, A. A., Irshad, M., Rahisuddin & Ahmad, A. Effect of parthenolide on growth and apoptosis regulatory genes of human cancer cell lines. *Pharm. Biol.* **53,** 104–109 (2015).
122. Gao, H. E., Sun, Y., Ding, Y. H., Long, J., Liu, X. L., Yang, M., Ji, Q., Li, Y. H., Chen, Y., Zhang, Q. & Gao,Y. D. Antineoplastic effects of CPPTL via the ROS/JNK pathway in acute myeloid leukemia. *Oncotarget* **8,** 38990–39000 (2017).
123. George, V., Kumar, D. & Kumar, R. Relative In Vitro Potentials of Parthenolide to Induce Apoptosis and Cell Cycle Arrest in Skin Cancer Cells. *Curr Drug Discov Technol* **13,** 34–40 (2016).
124. Jeyamohan, S., Moorthy, R., Kannan, M. & Arockiam, A. Parthenolide induces apoptosis and autophagy through the suppression of PI3K/Akt signaling pathway in cervical cancer. *Biotechnol Lett* **38,** 1251–60 (2016).
125. Kwak, S., Park, E. & Lee, C. Parthenolide induces apoptosis by activating the mitochondrial and death receptor pathways and inhibits FAK-mediated cell invasion. *Mol Cell Biochem* **385,** 133–44 (2014).
126. Lan, B., Wan, Y. J., Pan, S., Wang, Y., Yang, Y., Leng, Q., Jia, H., Liu, Y. H., Zhang, C. Z. & Cao, Y. Parthenolide induces autophagy via the depletion of 4E-BP1. *Biochem Biophys Res Commun* **456,** 434–9 (2015).
127. Sun, J., Zhang, C., Bao, Y.-L., Wu, Y., Chen, Z.-L., Yu, C.-L., Huang, Y.-X., Sun, Y., Zheng, L.-H., Wang, X. & Li, Y.-X. Parthenolide-induced apoptosis, autophagy and suppression of proliferation in HepG2 cells. *Asian Pac. J. Cancer Prev.* **15,** 4897–902 (2014).
128. Yu, H., Jung, J., Jeong, J., Cho, S. & Lee, J. Induction of apoptosis by parthenolide in human oral cancer cell lines and tumor xenografts. *Oral Oncol* **51,** 602–9 (2015).
129. Zhao, X., Liu, X. & Su, L. Parthenolide induces apoptosis via TNFRSF10B and PMAIP1 pathways in human lung cancer cells. *J. Exp. Clin. Cancer Res.* **33,** 3 (2014).
130. Liu, W., Wang, X., Sun, J., Yang, Y., Li, W. & Song, J. Parthenolide suppresses pancreatic cell growth by autophagy-mediated apoptosis. *Onco Targets Ther* **10,** 453–461 (2017).
131. Liu, Y., Kim, S., Park, Y., Lee, S. & Kim, S. Parthenolide promotes apoptotic cell death and inhibits the migration and invasion of SW620 cells. *Intes Res* **15,** 174–181 (2017).
132. Efferth, T., Gillet, J. P., Sauerbrey, A., Zintl, F., Bertholet, V., de Longueville, F., Remacle, J. & Steinbach, D. Expression profiling of ATP-binding cassette transporters in childhood T-cell acute lymphoblastic leukemia. *Mol Cancer Ther* **5,** 1986–94 (2006).
133. Liu, Z. L., Onda, K., Tanaka, S., Toma, T., Hirano, T. & Oka, K. Induction of multidrug resistance in MOLT-4 cells by anticancer agents is closely related to increased expression of functional P-glycoprotein and MDR1 mRNA. *Cancer Chemother Pharmacol* **49,** 391–7 (2002).
134. Estes, D., Lovato, D., Khawaja, H., Winter, S. & Larson, R. Genetic alterations determine chemotherapy resistance in childhood T-ALL: modelling in stage-specific cell lines and

correlation with diagnostic patient samples. *Br J Haematol* **139,** 20–30 (2007).

135. Kim, S. L., Kim, S. H., Park, Y. R., Liu, Y. C., Kim, E. M., Jeong, H. J., Kim, Y. N., Seo, S. Y., Kim, I. H., Lee, S. O., Lee, S. T. & Kim, S. W. Combined Parthenolide and Balsalazide Have Enhanced Antitumor Efficacy Through Blockade of NF-κB Activation. *Mol Cancer Res* **15,** 141–51 (2017).
136. Whipple, R. A., Vitolo, M. I., Boggs, A. E., Charpentier, M. S., Thompson, K. & Martin, S. S. Parthenolide and costunolide reduce microtentacles and tumor cell attachment by selectively targeting detyrosinated tubulin independent from NF-κB inhibition. *Breast Cancer Res* **15,** R83 (2013).
137. Zhang, D., Qiu, L., Jin, X., Guo, Z. & Guo, C. Nuclear Factor-kappaB Inhibition by Parthenolide Potentiates the Efficacy of Taxol in Non-Small Cell Lung Cancer In vitro and In vivo. *Mol Cancer Res* **7,** 1139–49 (2009).
138. Kim, S. L., Kim, S. H., Trang, K. T., Kim, I. H., Lee, S. O., Lee, S. T., Kim, D. G., Kim, S. B. & Kim, S. W. Synergistic antitumor effect of 5-fluorouracil in combination with parthenolide in human colorectal cancer. *Cancer Lett* **335,** 479–86 (2013).
139. Koprowska, K., Hartman, M., Sztiller-Sikorska, M. & Czyz, M. Parthenolide enhances dacarbazine activity against melanoma cells. *Anticancer Drugs* **24,** 835–45 (2013).
140. Liu, Y. C., Kim, S. L., Park, Y. R., Lee, S.-T. & Kim, S. W. Parthenolide promotes apoptotic cell death and inhibits the migration and invasion of SW620 cells. *Intest. Res.* **15,** 174 (2017).
141. Kim, S. L., Liu, Y.-C., Park, Y., Seo, S., Kim, S., Kim, I., Lee, S., Lee, S., Kim, D. G. & Kim, S. W. Parthenolide enhances sensitivity of colorectal cancer cells to TRAIL by inducing death receptor 5 and promotes TRAIL-induced apoptosis. *Int. J. Oncol.* **46,** 1121–30 (2014).
142. De Ford, C., Heidersdorf, B., Haun, F., Murillo, R., Friedrich, T., Borner, C. & Merfort, I. The clerodane diterpene casearin J induces apoptosis of T-ALL cells through SERCA inhibition, oxidative stress, and interference with Notch1 signaling. *Cell Death Dis* **7,** e2070 (2016).
143. Vilimas, T., Mascarenhas, J., Palomero, T., Mandal, M., Buonamici, S., Meng, F., Thompson, B., Spaulding, C., Macaroun, S., Alegre, M. L., Kee, B. L., Ferrando, A. D., Miele, L., Aifantis, I. Targeting the NF-κB signaling pathway in Notch1-induced T-cell leukemia. *Nat Med* **13,** 70–7 (2007).
144. Li-Weber, M., Palfi, K., Giaisi, M. & Krammer, P. H. Dual role of the anti-inflammatory sesquiterpene lactone: regulation of life and death by parthenolide. *Cell Death Differ.* **12,** 408–409 (2005).
145. Pei, S., Minhajuddin, M., D'Alessandro, A., Nemkov, T., Stevens, B. M., Adane, B., Khan, N., Hagen, F. K., Yadav, V. K., De, S., Ashton, J. M., Hansen, K. C., Gutman, J. A., Pollyea, D. A., Crooks, P. A., Smith, C. & Jordan, C. T. Rational Design of a Parthenolide-based Drug Regimen That Selectively Eradicates Acute Myelogenous Leukemia Stem Cells. *J. Biol. Chem.* **291,** 21984–22000 (2016).
146. Gach, K., Długosz, A. & Janecka, A. The role of oxidative stress in anticancer activity of sesquiterpene lactones. *Naunyn Schmiedebergs Arch Pharmacol* **388,** 477–86 (2015).
147. Escárcega, R., Fuentes-Alexandro, S., García-Carrasco, M., Gatica, A. & Zamora, A. The transcription factor nuclear factor-kappa B and cancer. *Clin. Oncol (R Coll Radiol)* **19,** 154–61 (2007).
148. Waring, P. & Mullbacher, A. Cell death induced by the Fas/Fas ligand pathway and its role in pathology. *Immunol. Cell Biol.* **77,** 312–317 (1999).
149. Walczak, H. Death receptor-ligand systems in cancer, cell death, and inflammation. *Cold*

Spring Harb. Perspect. Biol. **5,** a008698 (2013).

150. Peter, M. E., Hadji, A., Murmann, A. E., Brockway, S., Putzbach, W., Pattanayak, A. & Ceppi, P. The role of CD95 and CD95 ligand in cancer. *Cell Death Differ.* **22,** 549–59 (2015).
151. Holoch, P. A. & Griffith, T. S. TNF-related apoptosis-inducing ligand (TRAIL): A new path to anti-cancer therapies. *Eur. J. Pharmacol.* **625,** 63–72 (2009).
152. Park, S.-J., Bijangi-Vishehsaraei, K. & Safa, A. R. Selective TRAIL-triggered apoptosis due to overexpression of TRAIL death receptor 5 (DR5) in P-glycoprotein-bearing multidrug resistant CEM/VBL1000 human leukemia cells. *Int. J. Biochem. Mol. Biol.* **1,** 90–100 (2010).
153. Li-Weber, M., Palfi, K., Giaisi, M. & Krammer, P. Dual role of the anti-inflammatory sesquiterpene lactone: regulation of life and death by parthenolide. *Cell Death Differ* **12,** 408–409 (2005).
154. Ichim, G. & Tait, S. W. G. A fate worse than death: apoptosis as an oncogenic process. *Nat. Rev. Cancer* **16,** 539–548 (2016).
155. Guzman, M. L., Rossi, R. M., Karnischky, L., Li, X., Peterson, D. R., Howard, D. S. & Jordan, C. T. The sesquiterpene lactone parthenolide induces apoptosis of human acute myelogenous leukemia stem and progenitor cells. *Blood* **105,** 4163–9 (2005).
156. Steele, A. J., Jones, D. T., Ganeshaguru, K., Duke, V. M., Yohashangary, B. C., North, J. M., Lowdell, M. W., Kottaridis, P. D., Mehta, A. B., Prentice, A. G., Hoffbrand, A. V. & Wickremasinghe, R. G. The sesquiterpene lactone parthenolide induces selective apoptosis of B-chronic lymphocytic leukemia cells in vitro. *Leukemia* **20,** 1073–9 (2006).
157. Nikoletopoulou, V., Markaki, M., Palikaras, K. & Tavernarakis, N. Crosstalk between apoptosis, necrosis and autophagy. *Biochim. Biophys. Acta - Mol. Cell Res.* **1833,** 3448–3459 (2013).
158. Yang, C., Yang, Q. O., Kong, Q.-J., Yuan, W. & Ou Yang, Y.-P. Parthenolide Induces Reactive Oxygen Species-Mediated Autophagic Cell Death in Human Osteosarcoma Cells. *Cell. Physiol. Biochem.* **40,** 146–154 (2016).
159. Mariño, G., Niso-Santano, M., Baehrecke, E. H. & Kroemer, G. Self-consumption: the interplay of autophagy and apoptosis. *Nat. Rev. Mol. Cell Biol.* **15,** 81–94 (2014).
160. Nguyen, L., Papenhausen, P. & Shao, H. The Role of c-MYC in B-Cell Lymphomas: Diagnostic and Molecular Aspects. *Genes (Basel).* **8,** 116 (2017).
161. Ott, G., Rosenwald, A. & Campo, E. Understanding MYC-driven aggressive B-cell lymphomas: pathogenesis and classification. *Blood* **122,** 3884–91 (2013).
162. Chumduri, C., Gillissen, B., Richter, A., Richter, A., Milojkovic, A., Overkamp, T., Müller, A., Pott, C. & Daniel, P. T. Apoptosis resistance, mitotic catastrophe, and loss of ploidy control in Burkitt lymphoma. *J Mol Med* **93,** 559–72 (2015).
163. Diakos, C., Xiao, Y., Zheng, S., Kager, L., Dworzak, M. & Wiemels, J. L. Direct and Indirect Targets of the E2A-PBX1 Leukemia-Specific Fusion Protein. *PLoS One* **9,** e87602 (2014).
164. Mazieres, J., You, L., He, B., Xu, Z., Lee, A. Y., Mikami, I., McCormick, F. & Jablons, D. M. Inhibition of Wnt16 in human acute lymphoblastoid leukemia cells containing the t(1;19) translocation induces apoptosis. *Oncogene* **24,** 5396–400 (2005).
165. Nasim, S. & Crooks, P. Antileukemic activity of aminoparthenolide analogs. *Bioorg Med Chem Lett* **18,** 3870–3 (2008).
166. Viatour, P., Merville, M., Bours, V. & Chariot, A. Phosphorylation of NF-κB and IκB proteins: implications in cancer and inflammation. *Trends Biochem Sci* **30,** 43–52 (2005).
167. Cullen, S., Ponnappan, S. & Ponnappan, U. Redox-Regulated Pathway of Tyrosine Phosphorylation Underlies NF-κB Induction by an Atypical Pathway Independent of the

26S Proteasome. *Biomolecules* **5,** 95–112 (2015).

168. Gloire, G., Legrand-Poels, S. & Piette, J. NF-κB activation by reactive oxygen species: Fifteen years later. *Biochem Pharm.* **72,** 1493–505 (2006).
169. Alberts, B., Johnson, A., Lewis, J., Morgan, D., Raff, M., Roberts, K. & Walter, P. *Molecular Biology of the Cell*. (Garland Science, 2014).
170. Naugler, W. & Karin, M. NF-κB and cancer — identifying targets and mechanisms. *Curr Opin Genet Dev* **18,** 19–26 (2008).
171. Greten, F. & Karin, M. The IKK/NF-κB activation pathway — a target for prevention and treatment of cancer. *Cancer Lett* **206,** 193–9 (2004).